Adaptive protection scheme for microgrids based on SOM clustering technique☆

Seyyed Mohammad Ebrahim Ghadiri, Kazem Mazlumi *

Electrical Engineering Department, University of Zanjan, Zanjan 45371-38791, Iran

ARTICLE INFO

ABSTRACT

Microgrids are penetrating into the power systems at an unprecedented rate. The reason is the mutual economic and environmental benefits of microgrids, both for power grid utility and the consumers. Some special features of microgrids such as, the two main operational conditions called, islanded and grid-connected modes, and being composed of various types of distributed energy resources along with different uncertainties cause some tough challenges to protection and control systems. From the protection aspect, the coordination of overcurrent relays protection will become a difficulty, due to the extensive changes in the fault current levels sensed by these devices. In this paper, a new adaptive protection coordination scheme based on Self-Organizing Map (SOM) clustering algorithm is proposed for digital overcurrent relays equipped with several setting groups. Considering the similarity of mis-coordinated relay pairs for the clustering purpose, the proposed protection scheme focuses on solving the mis-coordination between main/backup relay pairs. As a case study, a modified IEEE 33-bus test system is used as a microgrid. In the case study, a synchronous distributed generation and two electric vehicle charging stations are installed. The results suggest that not only the proposed method is fully capable and flexible to significantly improve the mis-coordination of overcurrent relay pairs, but it can also ameliorate the operating time of relay.

1. Introduction

These days, electrical power demand is increasing faster than any time and responding to these demands, needs unprecedented expansion of power supply. A simple solution is to build traditional power plants, which causes various problems such as:

(a) imposing high cost and long time to build,
(b) huge power loss in transmission lines,
(c) low efficiency and less reliability,
(d) growing concerns about global warming and environmental pollution due to increasing emissions of greenhouse gases [1].

Another solution is employing Distributed Energy Resources (DERs) in small scales and large quantities at Low Voltage (LV) and Medium Voltage (MV) distribution levels, especially near to the load centers [2–5].

This will solve the mentioned problems, but entails other issues in power management, safety, protection, and control systems because of DERs intermittent and uncertainties, again demanding attention to handle these problems.

Microgrid concept has been created in order to address these issues; it is usually an LV or MV distribution power network which includes Distributed Generations (DGs) and Energy Storage Systems (ESSs) as DERs. It is equipped with a centralized/decentralized control unit [6] and a proper protection system.

One of the most important features of a microgrid is the fact that it can operate in both grid-connected and islanded modes. Normally microgrids operate as grid-connected and they have power exchanges with the upstream network. If any disturbance happens in the upstream network, the microgrid almost simultaneously changes the operation into the islanded mode [7] and provides uninterrupted high-quality power at least for the main loads [8].

Implementation of microgrids bring some important protection challenges to the existing protection systems which are mainly non-directional overcurrent relays.

- The first challenge is the bidirectional power flow [9] in microgrids due to the use of multiple DERs.
- Another major issue is the dynamic operation modes of microgrid under the inflow and outflow of different types

of DERs. This issue causes different short circuit levels which are supposed to be seen by protective devices [10,11]. The whole power system may be exposed to danger in this situation.

- The last protection challenge is the fact that a microgrid mainly consists of inverter base DERs and these units have a weak short circuit feeding capability; thus they do not change the short circuit level very much when the microgrid is operating in the grid-connected mode. In this case, the upstream side feeds the required short circuit current required by protective devices; however when the microgrid is operating in islanded mode, the low fault current of these types of DERs is almost invisible to the protective devices [12] and the protection system simply fails to identify the fault current.

Different approaches have been developed so far to offer a proper protection method for microgrids or DG base power networks with some of them being described in the following section.

Integrating Superconducting Fault Current Limiters (SFCLs) in order to reduce the fault current produced by DERs has been discussed in [13]. Using Fault Current Limiters (FCLs) incorporated with adjustment of new relay settings has been presented in [14]. The main drawbacks and challenges of using FCLs would be the high implementation cost, intermittent DERs, and dynamic operation modes of microgrids as mentioned earlier.

A microgrid protection strategy based on microprocessor relays for both grid-connected and islanded mode has been reported in [15]. Applying differential and voltage protection methods for islanded microgrids using communication networks has been studied in [16]. The communicational failure should be considered in these types of protection.

In [17], a method has been proposed in which through dividing the distribution network into several zones, a protection coordination was calculated for each zone independently while the zones were capable of operating in islanded-mode.

In [18,19], using dual setting directional overcurrent relays, an adaptive protection has been proposed based on communications for networks under DG penetrations and microgrids capable of both grid-connected and islanded mode operation. The main problems are the actual cost to implement these types of dual setting directional overcurrent relays in the network and the need for readjusting relay settings due to DG uncertainties and different operation scenarios of the microgrid.

In [20], an adaptive protection scheme has been proposed for power networks under penetration of DERs. This research benefits from offline and online phases. Initially in the offline phase, dominant network topologies are selected and the optimized relay settings are calculated for each one. Then, in the online phase these, dominant network topologies are recognized by a fuzzy logic block after which the respective relay settings are communicated to the relays.

Classification and clustering techniques have been used in several studies, in order to detect faulty conditions of the network, fault type and fault locations [21–24].

In [25], based on k-means clustering technique, an adaptive protection method has been presented. The method reduces all similar operating topologies of a network into a few clusters equal to the number of setting groups of digital overcurrent relays. Next, the protection coordination problem in each cluster is optimized for all cluster members. Finally, depending on the topology of the network is operating in, the desired relay settings are selected for each overcurrent relay by communication links among substations. By analyzing the objective function (OF) and the final results, the main target of the paper seems to be only achieving a shorter operation time for overcurrent relays. Despite the fact that the proposed method is actually successful

in this area of interest, the paper does not give assurance about optimized coordination between main/backup relay pairs based on the objective function defined in the paper, which is one of the main targets for any overcurrent relay based protection system. Furthermore, estimation with large errors in time dial setting value by considering it as unity in the operation time formula of the main/backup overcurrent relays, in order to cluster the topologies based on general time intervals, leads to increased probability of incorrect conclusion about the availability of the clustering method in series connected power lines (radial networks) in comparison with the other proposed scheme in the paper.

Table 1 summarizes the microgrid and DG based power network protection schemes along with data mining-based protection methods, their corresponding applied methods, and advantages\limitations of each one.

In this research, a new adaptive protection method based on Self-Organizing Map (SOM) clustering technique for a microgrid is presented. Multiple scenarios are determined as different operational conditions of the studied microgrid. The adaptive approach is defined in three phases. Initially, based on a conventional protection scheme, protection results are analyzed for each scenario. Then, based on the results, using SOM clustering technique and given the similarities of faulty coordinated overcurrent relay pairs, all defined scenarios are divided into several clusters in the second phase as well as several sub-clusters in the third phase.

For each cluster, the proper relay settings are obtained by a specific approach, so when the microgrid changes its operation mode into another scenario, the corresponding relay settings of the related cluster are applied to overcurrent relays.

One of the important advantages of this paper is the comparison of both protection coordination conditions of overcurrent relays during the implementation of the protection scheme. Initially, the main goal is to reduce the overall magnitude of mis-coordination intervals between the overcurrent relay pairs as much as possible for each scenario, which is achieved by introducing a new index in this research. In the next step, the operating time of these relays for the faults exactly in front of the main overcurrent relay is analyzed to make sure relays have not become slower due to the settings applied.

Based on the selected communication method, implementation of the proposed adaptive protection scheme is possible in two different ways which are explained in the following: (obviously each one has its own advantages and limitations):

- Centralized control unit: In communication protocols such as IEC 61850 [20], relays are connected to a central control unit which continuously monitors the power network and communicates the corresponding settings to each relay. The positive effect of this type of communication is that the number of defined clusters for the operation scenarios in the power network is almost unlimited; thus, the number of clusters are determined as long as the protection coordination conditions are satisfied completely. The negative effect of this approach, however, is the actual cost of implementing this system; more importantly, centralized communication protocols suffer from failure occurrence which puts the entire protection system in danger.
- Decentralized approach: In this approach a decentralized communication protocol such as peer-to-peer protocol [25] is employed for substation-to-substation communications. Each substation reports its status to the neighboring substations and based on these reports the correct settings are selected for each relay. The positive effect of the mentioned method is the cost efficiency and the fact that failure in one communication link does not affect the performance of

Table 1
Microgrid and DG-based power network protection schemes and data mining-based protection methods.

Reference(s)	Protection scheme	Applied methods	Advantages/Limitations
[13,14]	Fault current reduction by external devices, adaptive and non-adaptive protection schemes	FCLs, SFCLs, directional and non-directional overcurrent relays	High cost, impedance value selection is challenging due to DG uncertainties, basically the number of these devices (FCLs) rises by increase in the number of DGs.
[15]	Microgrid protection	Microprocessor-based relays	Adaptive protection schemes or communicational links are not required, long time delays in clearing faults.
[16]	Microgrid protection	Differential relays, voltage measurement unit	Accurate fault detection and high costs for differential relays as well as lower performance for voltage measurements and cost efficiency for voltage measurement scheme, both methods need communicational links.
[17]	Adaptive protection scheme, fault type detection and location, network zoning approach	Risk analysis, Artificial Neural Networks (ANNs), load shedding, computer-based relays	Zones are capable of operating in islanded mode, determining the location of the protective devices by risk analysis, fault type detection and location is challenging in DG presence.
[18,19]	Adaptive protection scheme, microgrid protection	Dual setting directional overcurrent relays	The protection scheme is mainly based on communicational links, readjusting of relay settings in different DG uncertainties is required, implementation costs should be considered.
[20]	Adaptive protection scheme	Microprocessor-based relays, fuzzy based approach	High cost of centralized control unit, also communication failure should be considered, malfunction of implemented fuzzy rule base in identification of topologies other than the defined dominant network topologies.
[22–24]	Fault type detection, location and classification, DC protection schemes	Unit and non-unit protection, adaptive wavelet transform, intelligent based method	Unit protection methods are able to protect specific parts of the DC network, non-unit protection schemes are able to protect different constituents of DC systems non-specifically and can be used as backup protection of unit protection methods, wavelet transform requires high frequency sampling and therefore high cost, communication failure in unit protection may lead to some challenges in fault detection and isolation, intelligent based methods are highly dependable on training data collection.
[25]	Adaptive protection scheme, data mining-based protection scheme	Digital overcurrent relays, k-means clustering method	Different operational topologies of the power network are clustered by general time delays of relays and general time intervals of relay pairs, clusters are equal to the setting groups of digital relays, possible decentralized communication links, the OF does not guarantee optimized coordination of the relay pairs, time dial settings of relays are considered as unity for clustering which may cause some difficulties in radial parts of a power network, only single-contingency topologies are analyzed and uncertainties of DGs or generators are not considered, optimal protection conditions of clusters are challenging in huge power networks due to many different topological changes.
Current paper	**Adaptive protection scheme, microgrid protection, data mining-based protection scheme**	**Digital overcurrent relays, SOM clustering method, new index-based protection condition evaluation, inverter based DGs**	**Different operation scenarios of microgrid including islanded/grid-connected modes and DG uncertainties are considered for the clustering purpose, EV charging stations are considered for simulation as inverter based DGs, scenarios are selected as multi-contingencies, clustering is independent of network topology and it is based on mis-coordination time interval between main/backup relay pairs of each scenario (flexible method), the proposed method is categorized in three phases in order to maximize the efficiency of the results, decentralized communicational approach such as peer-to-peer protocol is applicable (cost efficiency), the chosen OF optimizes both operating time of the relays and coordination conditions between relay pairs, introducing a new index to analyze the protection coordination conditions between relay pairs in massive power networks.**

the protection system. The only limitation of this method is the fact that digital overcurrent relays have limited available setting groups to be used (usually 2, 4, or 8).

Based on the considered operation scenarios, the studied microgrid as well as cost efficiency, decentralized communication approach is chosen and therefore the number of selected clusters for the proposed adaptive scheme is limited to the number of setting groups of digital overcurrent relays. Eventually, it is notable that Matlab [26] and Digsilent PowerFactory [27] software applications have been employed in this research while for the test case, modified IEEE 33-bus system as a microgrid has been used. The results guarantee the flexibility and efficiency of the proposed protection scheme in achieving the determined targets.

This article is organized as follows:

In Section 2 overcurrent relays coordination problem is discussed. Section 3 briefly reviews the SOM algorithm. Section 4 introduces the proposed adaptive protection scheme. Test case study is described in Section 5. Section 6 presents the results of simulation, and eventually Section 7 concludes the paper.

2. Protection coordination problem formulation

Inverse time overcurrent relays have two factors to be adjusted, Time Dial Setting (TDS) and pick-up current. In order to coordinate a set of these relays together in a huge interconnected power network, correct calculation of TDS and pick-up current values becomes increasingly complicated due to protection considerations. It means that the protection coordination issue between these overcurrent relays is an optimization problem.

This optimization is based on two major subjects: it should consider the relays tripping time to be as fast as possible on one hand and should maintain the main/backup relay pairs correctly coordinated on the other. Thus, the great importance of selecting an appropriate OF for protection coordination is an undeniable matter.

Many works have been already undertaken to introduce an efficient OF for this problem [28–30]. As discussed in [31], the OF expression (1) can be minimized by a genetic algorithm. Note

that the selected OF is a non-linear programming problem whose optimization by genetic algorithm finally leads to gaining a set of TDS values for overcurrent relays in a way that both the operating time of the relays and coordination time between relay pairs are minimized.

$$OF = \alpha_1 \sum (t_i)^2 + \alpha_2 \sum \left(\Delta t_{mbj} - \beta_2 \left(\Delta t_{mbj} - |\Delta t_{mbj}|\right)\right)^2 \quad (1)$$

where α_1, α_2, and β_2 represent the weight coefficients and are used to establish a balance in the equation between minimizing the operating time of the relays and optimizing the coordination time between the main and backup relay pairs. Thus, their values play an important role in this formula [30]. t_i is the operating time of the ith overcurrent relay due to the fault exactly in front of the respected overcurrent relay. The Δt_{mbj} value is calculated for the jth main/backup relay pair as follows [32]:

$$\Delta t_{mbj} = t_{bj} - t_{mj} - CTI \quad (2)$$

t_{mj} is the operating time of the main relay in jth relay pair for the fault exactly in front of it and t_{bj} is the operating time of backup pair of the mentioned main relay. The coordination time interval for the main and backup relay pairs is called CTI which is usually considered within 0.2–0.5 s.

Calculation of t_i is considered as [33,34]:

$$t_i = \frac{k}{\left(\frac{I_{shc}}{I_{pi}}\right)^n - 1} \times TDS_i \quad (3)$$

The above expression offers the operation time value (t_i) for the fault current (I_{shc}) exactly in front of the corresponding relay. I_{pi} is the ith relay's pick-up current value. k and n denote the relay constants whose values are 0.14 and 0.02, respectively, for a standard time inverse (SI) overcurrent relay [34]. TDS_i is called the time dial setting of the ith overcurrent relay.

The constraints defined for calculating t_i value are [33]:

$$TDS_{min} < TDS_i < TDS_{max} \quad (4)$$

$$I_{pi}^{min} < I_{pi} < I_{pi}^{max} \quad (5)$$

$$\Delta t_{mb} \geq 0 \quad (6)$$

In constraint (4), TDS_i should be picked from 0.05 (TDS_{min}) up to 2 (TDS_{max}) in 0.001 steps. Based on (5) the value for I_{pi}, should be taken somewhat between the maximum load current (I_{pi}^{min}) and the minimum short circuit current (I_{pi}^{max}) which is sensed by the mentioned overcurrent relay. In order to facilitate the calculations in this paper, it is assumed that the pickup currents of overcurrent relays are pre-optimized, thus making (3) a linear programming problem. Constraint (6) reminds that the operational time difference between the main and backup relay pairs needs to be equal to or more than zero; otherwise, the related relay pair suffers from mis-coordination.

The constraints of protection coordination conditions of overcurrent relays in this research are determined as follows:

(a) Optimized coordination between main/backup overcurrent relay pairs ($\Delta t_{mb} \rightarrow 0^+$). The proposed adaptive protection method lays the main focus on this constraint given its importance.

(b) Operational time of the overcurrent relays should be as short as possible when dealing with faults as the main protective relay ($t_i \rightarrow 0$).

3. SOM

The typical question that might occur for anyone reading the paper is, why SOM?

Mostly in protective systems of massive power distribution networks, many overcurrent relays are installed; in some cases, this leads into even more main/backup relay pairs, especially for interconnected networks. The adaptive protection approach suggested in this research uses clustering techniques for different operation scenarios, such as islanded/grid-connected modes of microgrid and connection/disconnection and different uncertainties of DGs. In order to cluster these scenarios, a large input data set of a defined characteristic of overcurrent relay pairs is chosen. The mentioned characteristic and the input data set are discussed completely in the next section of the paper.

Kohonen map or better known as SOM is a famous practical clustering technique when dealing with a large input data set [35,36]. SOM was first introduced by Kohonen [37]; it is an unsupervised type of ANN [38] which learns to non-linearly build a low dimensional output grid from a high dimensional input data through training [39].

Neurons in this method are usually distributed on a two-dimensional rectangular or hexagonal grid (lattice). A weight vector with the same size of the input data vector is randomly specified for each neuron in order to adapt themselves to the input data space [39].

The method benefits from competitive learning procedure in which every input data vector dedicates itself to all neurons of the output grid. The neuron with the closest distance to that input vector is fired as the winner neuron, after which the weight vector of the neuron and the neighbors will be updated. Note that the update rate differs between the winner, the nearer, and the farther neighbor neurons. The shape of the initially determined map changes through updating the weight vectors of neurons. Then, the mentioned procedure is executed again which continues many times until the specified iteration number is reached [39].

As this cycle continues, the rate of these updates decreases both for the winner neuron and its neighbors [40]. It is because in each epoch, the need for exploiting the input space outweighs the importance of its exploration.

After selecting the winner neuron, SOM clustering algorithm uses the following equation [39,41]:

$$\omega_j(t+1) = \omega_j(t) + \eta(t)h_{ij}(x,t)(x - \omega_j(t)) \quad (7)$$

The term x stands for input data vector and ω_j refers to the weight vector of the jth neuron, $\eta(t)$ is the learning rate of the algorithm, and $h_{ij}(x,t)$ denotes the neighborhood function between the winner neuron (i) and the neighbor neuron (j) which is dependent on the distance between these two.

The $h_{ij}(x,t)$ function can be expressed as Gaussian [39]:

$$h_{ij}(x,t) = e^{\left(-\frac{d_{ij}^2}{2\sigma(t)^2}\right)} \quad (8)$$

The d_{ij} indicates the distance parameter between the winner neuron (i) and the neighbor neuron (j). Note that different functions can be used such as Euclidean distance, link distance or Manhattan distance in order to calculate d_{ij}.

$\eta(t)$ as the learning rate function and $\sigma(t)$ as the neighborhood radius function, must be considered as decreasing of time functions [37]; for instance $\eta(t)$ and $\sigma(t)$ can be exponential [36] as follows:

$$\eta(t) = \eta_0 e^{\left(-\frac{t}{\tau}\right)} \quad (9)$$

$$\sigma(t) = \sigma_0 e^{\left(-\frac{t}{\tau_0}\right)} \quad (10)$$

where, η_0, σ_0, τ, and τ_0 represent constant variables.

4. Proposed adaptive protection scheme

As mentioned in Section 1, from the protection aspect at the distribution level which basically includes a set of overcurrent

relays, several important obstacles occur when employing microgrids. Most of these problems are caused by different operational conditions a microgrid is defined to work in. Finally, these uncertainties and operational scenarios lead to different fault current levels. Mostly, these fault currents will not be seen by overcurrent relays. This research proposes an adaptive protection scheme to address the challenges in protection of microgrids.

4.1. Prerequisites of the proposed method

In order to explain the proposed adaptive protection scheme further, five important indices should be defined well.

4.1.1. Mis-coordination Time
To describe other indices, the Mis-coordination Time (MT) index should be defined as follows:

$$MT_j = \frac{\left(\Delta t_{mb_j} - \left|\Delta t_{mb_j}\right|\right)}{2} \tag{11}$$

where, MT_j refers to mis-coordination time value of the jth main/backup overcurrent relay pair. It is obvious that MT_j has always a negative or zero value; as the negative value grows larger, the coordination between jth relay pair is deteriorated. On the other hand, if the mentioned relay pairs are somehow coordinated ($\Delta t_{mb} > 0$), MT_j becomes zero.

4.1.2. Total Mis-coordination Time
In this paper, in order to easily analyze the protection coordination condition between main/backup relay pairs in each operation scenario, a new index is introduced based on the presence of numerous overcurrent relay pairs in the studied microgrid. The index stands for Total Mis-coordination Time (TMT) value and it is expressed for the nth scenario (Sc_n) as follows:

$$TMT_{Sc_n} = \sum_{j=1}^{k} MT_j \tag{12}$$

where, k refers to the number of the overcurrent relay pairs in the Sc_n. Note that, based on the expression, TMT_{Sc_n} always gets negative or zero as well; its larger negativity indicates aggravated coordination between the relay pairs of the Sc_n. Thus, the protection coordination condition between the relay pairs in the Sc_n improves only if the absolute value of the TMT_{Sc_n} diminishes ($TMT_{Sc_n} \to 0^-$).

4.1.3. Mis-coordinated Relay Pairs Matrix
The Mis-coordinated Relay Pairs Matrix (MRPM) is created to be used as the input data set for training the SOM clustering algorithm. MRPM consists of MT index values of main/backup relay pairs for the set of selected scenarios, and is calculated by applying a particular TDS and pickup current settings to all selected scenarios. It captures the number of columns as the number of the chosen scenarios and the number of rows as the number of all possible main/backup relay pairs in the power network.

Almost expectedly, applying the same relay settings to all selected scenarios makes some of main/backup relay pairs coordinated and while causing mis-coordination among some other ones; hence the MRPM consists of negative and zero elements.

If the selected set of scenarios (S) for clustering is considered as:

$$S = \{Sc_1, Sc_2, \ldots, Sc_n\} \tag{13}$$

Then the MRPM is expressed as follows:

$$MRPM = \begin{bmatrix} MT_{11} & \cdots & MT_{1n} \\ \vdots & \ddots & \vdots \\ MT_{k1} & \cdots & MT_{kn} \end{bmatrix} \tag{14}$$

Note that the matrix includes all possible main/backup relay pairs in all specified scenarios of the case study as the number of the rows. Typically, the number of these relay pairs is not the same in all scenarios, suggesting that some of the relay pairs which are present and active in several scenarios do not exist in other ones. Thus, the related matrix value for any absent relay pair in each scenario is also considered as zero.

4.1.4. Cluster Mis-coordination Condition Matrix
Once the clustering procedure ends for S as in (13), the ith cluster of scenarios as the subset of S is expressed as:

$$Cluster_i \subset S \Rightarrow Cluster_i = \left\{Sc_{n_1}, Sc_{n_2}, \ldots, Sc_{n_m}\right\} \tag{15}$$

where, Sc_{n_m} stands for the mth scenario as the member of the set of $Cluster_i$.

The Cluster Mis-coordination Condition Matrix (CMCM) which is required for determining the next index is described for the ith cluster as a row matrix:

$$CMCM_{Cluster_i} = \left[TMT_{Sc_{n_1}}, TMT_{Sc_{n_2}}, \ldots, TMT_{Sc_{n_m}}\right] \tag{16}$$

Based on definition of (16), CMCM is mostly a negative matrix. Note that a particular TDS and pick-up current settings are used to calculate TMT values of the matrix.

4.1.5. The Most Effective Scenario
The Most Effective Scenarios (TMESs) are defined in order to accelerate and facilitate the calculation of the optimization problem for each cluster.

After forming the CMCM, the column with the most negative value among other matrix elements belongs to TMES of the related cluster.

Considering CMCM as (16), TMES of the ith cluster is as the following expression:

$$TMES_{Cluster_i} = Sc_{n_l} \Longleftrightarrow TMT_{Sc_{n_l}} = min\left\{CMCM_{Cluster_i}(m)\right\} \tag{17}$$

where, $CMCM_{Cluster_i}(m)$ represents the mth column of $CMCM_{Cluster_i}$ and Sc_{n_l} is the lth scenario of $Cluster_i$.

Note that since TMES has the most negative value among other members of the CMCM, it has the worst protection coordination between the main/backup relay pairs and needs further attention. Thus, the protection coordination settings of relays for the cluster members are based on optimized relay settings of the related TMES. This suggests that TMESs indeed represent their related cluster from the protection coordination problem aspect.

4.2. The procedure of the proposed method

The proposed adaptive protection scheme which is defined and discussed completely as an algorithm in the rest of this section is illustrated in Fig. 1 as a flowchart.

4.2.1. Phase one (Conventional Protection Scheme)
Step 1: In the beginning, among all defined scenarios, a desired one is chosen as the base scenario. All required information about the chosen scenario which basically consists of the short circuit current results seen by overcurrent relays as well as a list of main and backup relay pairs is gathered. By applying the genetic algorithm to (1), the optimized TDS settings are gained for overcurrent relays of the base scenario. The protection coordination conditions (described in Section 2) are checked for the base and then for all specified scenarios of the microgrid. It is notable that, to simplify the analyses for each scenario in this paper due to the hugeness of the studied microgrid, TMT index is used for checking coordination between relay pairs, while the average tripping time of the relays is chosen to examine the operating time of the relays.
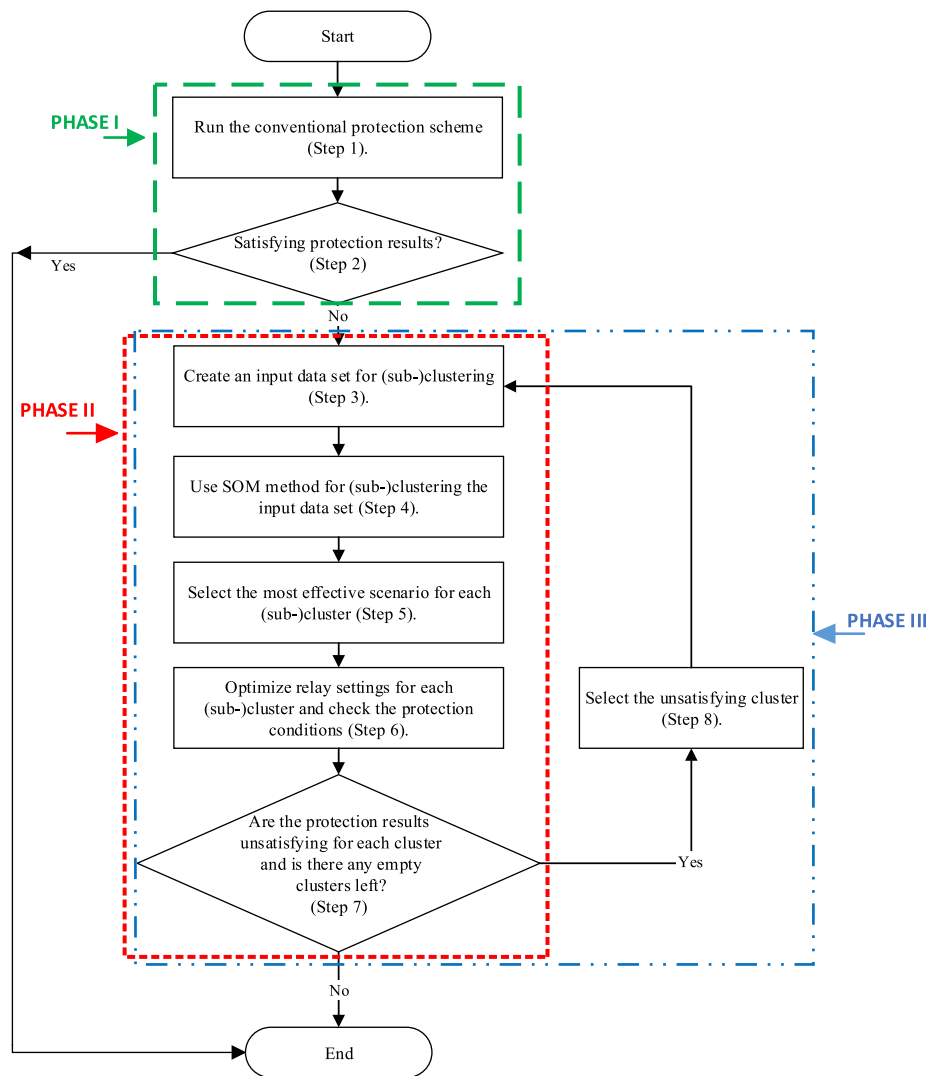
Fig. 1. Proposed adaptive protection scheme.

Step 2: Analyzing the protection coordination conditions between different scenarios by applying the same TDS and pick-up current settings obtained in the first step will give us a general overview about the next phase. Are the two protection coordination conditions satisfied for all scenarios? If the answer is positive, then basically the selected test network and defined scenarios will not need any special protection scheme. However, if the answer is negative, or the protection coordination conditions do not seem to be satisfying enough, an adaptive protection scheme is required which leads us to the second phase and next step of the proposed protection method. Phase one ends here, which is mainly called as the conventional (non-adaptive) protection scheme.

4.2.2. Phase two (Clustering Method)

Step 3: By considering the gained TDS and pick-up current setting values for the base scenario in step 1, the MRPM is created and used as an input data set for training SOM clustering algorithm. Note that, in step 3 of phase 2, the whole set of the defined scenarios in the case study has to be selected (see Section 4.1.3).

Step 4: Clustering procedure is done in this step using the MRPM created in the previous step. Note that, the number of clusters is dependent on the available setting groups of the digital overcurrent relays [25]. Thus, the size of the ordered map or the lattice called must be considered as any desired multiplication

of numbers equal to the number of relay setting groups. Note that giving different multiplications may cause different results. Therefore, it is recommended to try different multiplications in order to obtain the better results.

Step 5: By now, SOM has divided all scenarios into some clusters. For each cluster, based on the existing scenarios and recently relay settings applied to calculate MRPM (in step 3), the respective CMCM is created (presented as Section 4.1.4). After analyzing the CMCM in each cluster, the related TMES is selected by the description (described as Section 4.1.5).

Step 6: Now that TMES has been chosen for each cluster, the required information is gathered for each TMES, and OF is optimized for each one through genetic algorithm. Then the TDS and pick-up current values are gained for each TMES. Finally, the previously mentioned protection coordination conditions are checked for all cluster members by applying the obtained relay settings of the respected TMES.

Step 7: In each cluster, the results are compared with earlier outcomes from the conventional protection scheme (phase one). Analysis of the results will also show improvements. If the results were all satisfying for each cluster, then the algorithm ends right here. Conversely, results of phase two might not be satisfying enough, thus more considerations are needed. Note that after SOM clustering procedure ends, in some cases, there might be some neurons that were not used at all; these neurons which can
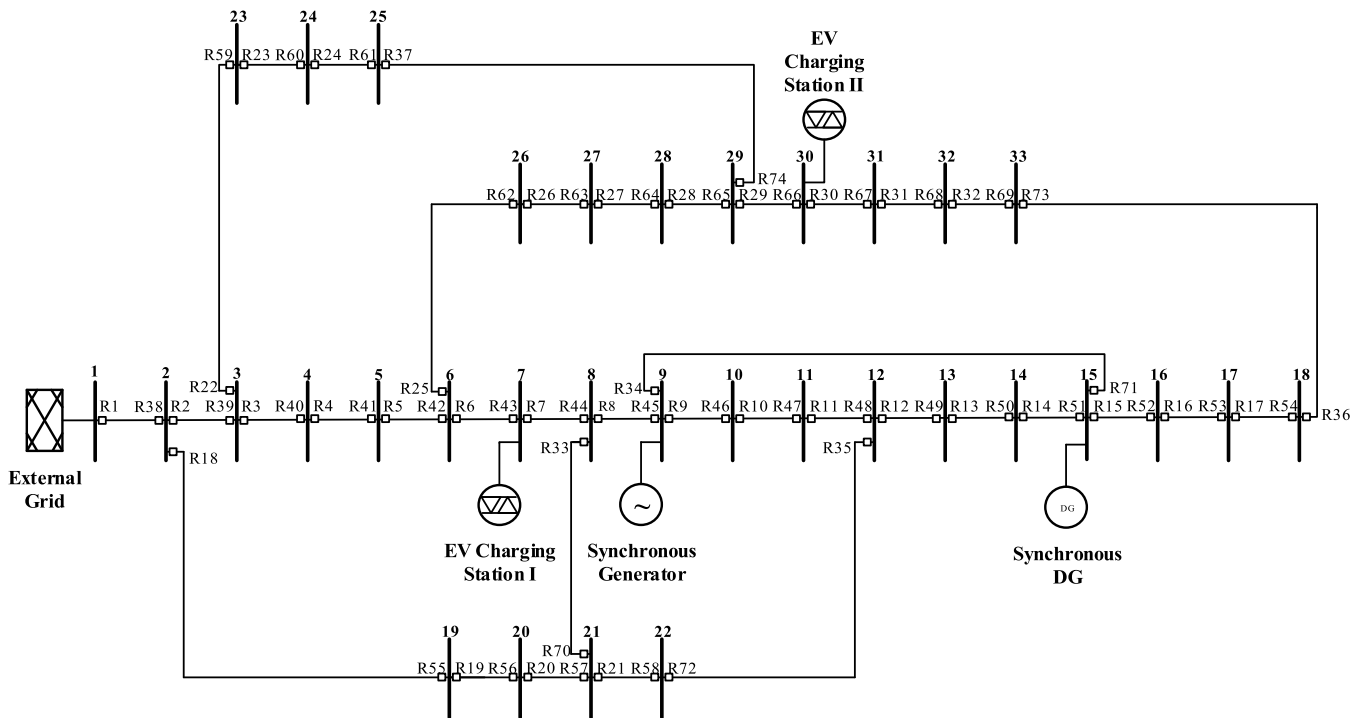
Fig. 2. Modified IEEE 33-bus case study.

be called as loser neurons will not form any clusters. Hence in these cases where the final results are not satisfying and there are still some remaining empty clusters to be used, the proposed protection method steps further by creating two or more sub-clusters (according to the limitation of the relay setting groups) out of each unsatisfying cluster.

4.2.3. Phase three (Sub-clustering Method)

Step 8: This phase is very similar to the second one; assuming there is only one empty cluster (loser neuron) left, the cluster with the worst protection coordination conditions is picked as the unsatisfying cluster. Then, the whole second phase process (step 3 to step 7) is repeated again, this time only the set of selected scenarios in step 3 is the set of members of the unsatisfying cluster. Also, the calculated TDS and pick-up current settings of the unsatisfying cluster in step 6 of phase two is used in step 3 and step 4 of phase three. Note that the lattice size for SOM clustering in this phase is selected based on the limitations. Phase three is also called as sub-clustering method.

As can be seen, phase three is a cycle which can be repeated until one of the conditions in step 7 terminates the procedure. In any case, if possible, applying the third phase will show great improvements in the results.

5. Test case study

Modified IEEE 33-bus test system [42] is used as a microgrid model as shown in Fig. 2. The nominal voltage of the grid is 12.66 kV and its original load consumption is 3.715 MW and 2.3 MVAR. There are two Electric Vehicle (EV) charging stations at the 7th and 30th buses. The charging station at bus 7 is considered to be able to charge/discharge 24 EVs with 50 kWh battery capacities while the other one at bus 30 does the same for 20 EVs [43,44]. There is a synchronous DG connected to bus number 15 with full capacity of 2.5 MW. Since we are not going to deal with controlling issues of the microgrid, we assume there is a PV bus including a synchronous generator at bus 9 which is capable

of keeping the entire system alive in the worst case scenarios especially in the islanded mode.

Note that there are 74 directional overcurrent relays in the proposed network, allowing for possible 100 main/backup relay pairs in this case study.

The selected scenarios consist of:

(a) Islanded and grid connected modes;
(b) Connected and disconnected modes for synchronous DG at bus number 15;
(c) Five operation statuses for each EV charging station, including: full-charge, full-discharge, half-charge, half-discharge, and out-of-service.

By combining the above operation conditions, a sample set of 68 scenarios is formed, which can be seen in Table 2.

6. Simulation and results

6.1. Phase one (Conventional Protection Scheme)

The scenario which includes the microgrid connected to the upstream network, disconnected synchronous DG, and both EV charging stations in out-of-service status, is selected as the base scenario in this paper and is considered as the first scenario in Table 2.

Note that each scenario in this paper is simulated in DIgSILENT PowerFactory software environment. Next, the required short circuit data for the fault current exactly in front of the overcurrent relays are also achieved by the mentioned software. The type of the short circuit is considered as the maximum three-phase fault current.

In the next step, in order to minimize OF (described in Section 2) and achieve the best possible results for relay settings in the base scenario, the genetic algorithm is used as an optimization tool with the parameters of 2000 population size and 5000 generations. In this research, α_1, α_2, and β_2 are selected as 1, 2, and 100 respectively in order to achieve the best outcome [31], also CTI is considered as 300 ms.

Table 2
All defined scenarios.

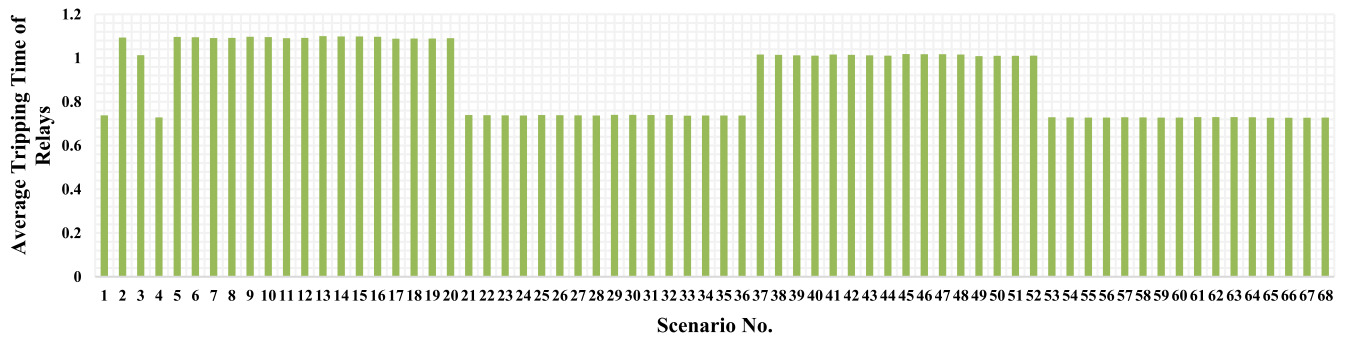| Scenario	Operation modes of microgrid		EV charging station 1				EV charging station 2				Synchronous DG
	Grid-connected	Islanded	Full charge	Full discharge	Half charge	Half discharge	Full charge	Full discharge	Half charge	Half discharge	
1	✔										
2		✔									
3		✔									✔
4	✔										✔
5		✔	✔								
6		✔			✔						
7		✔		✔							
8		✔				✔					
9		✔					✔				
10		✔							✔		
11		✔						✔			
12		✔								✔	
13		✔	✔				✔				
14		✔			✔		✔				
15		✔	✔						✔		
16		✔			✔				✔		
17		✔		✔				✔			
18		✔				✔		✔			
19		✔		✔						✔	
20		✔				✔				✔	
21	✔		✔								
22	✔				✔						
23	✔			✔							
24	✔					✔					
25	✔						✔				
26	✔								✔		
27	✔							✔			
28	✔									✔	
29	✔		✔				✔				
30	✔				✔		✔				
31	✔		✔						✔		
32	✔				✔				✔		
33	✔			✔				✔			
34	✔					✔		✔			
35	✔			✔						✔	
36	✔					✔				✔	
37		✔	✔								✔
38		✔			✔						✔
39		✔		✔							✔
40		✔				✔					✔
41		✔					✔				✔
42		✔							✔		✔
43		✔						✔			✔
44		✔								✔	✔
45		✔	✔				✔				✔
46		✔			✔		✔				✔
47		✔	✔						✔		✔
48		✔			✔				✔		✔
49		✔		✔				✔			✔
50		✔				✔		✔			✔
51		✔		✔						✔	✔
52		✔				✔				✔	✔
53	✔		✔								✔
54	✔				✔						✔
55	✔			✔							✔
56	✔					✔					✔
57	✔						✔				✔
58	✔								✔		✔
59	✔							✔			✔
60	✔									✔	✔
61	✔		✔				✔				✔
62	✔				✔		✔				✔
63	✔		✔						✔		✔
64	✔				✔				✔		✔
65	✔			✔				✔			✔
66	✔					✔		✔			✔
67	✔			✔						✔	✔
68	✔					✔				✔	✔

Fig. 3. Relays average tripping time for each scenario in conventional protection method (phase 1).

Table 3
TMT index values for each scenario based on conventional protection scheme (phase 1).

Scenario	TMT (s)	Scenario	TMT (s)	Scenario	TMT (s)	Scenario	TMT (s)
1	−0.00042	18	−13.894423	35	−0.0112834	52	−12.542793
2	−13.916923	19	−13.892341	36	−0.006487	53	−0.156998
3	−12.554439	20	−13.90071	37	−12.570339	54	−0.1624591
4	−0.1682349	21	−0.0061305	38	−12.562008	55	−0.1738456
5	−13.937856	22	−0.0031238	39	−12.547248	56	−0.1797125
6	−13.926819	23	−0.0022498	40	−12.540743	57	−0.1646304
7	−13.899053	24	−0.0069939	41	−12.563925	58	−0.164838
8	−13.907457	25	−0.0148034	42	−12.55899	59	−0.1752465
9	−13.930498	26	−0.0057074	43	−12.54993	60	−0.1833202
10	−13.92359	27	−0.0036333	44	−12.545744	61	−0.1543259
11	−13.903848	28	−0.010066	45	−12.57997	62	−0.1591123
12	−13.910153	29	−0.0181563	46	−12.571632	63	−0.1549208
13	−13.951224	30	−0.0164257	47	−12.575022	64	−0.1598458
14	−13.940325	31	−0.0090026	48	−12.566624	65	−0.1940987
15	−13.944487	32	−0.0072047	49	−12.532243	66	−0.1886799
16	−13.933485	33	−0.0191556	50	−12.538654	67	−0.1862461
17	−13.886081	34	−0.0135	51	−12.536338	68	−0.1805802
Average TMT		**−6.6632 s**					

The results of the TDS and pick-up current settings of each overcurrent relay are available in Appendix A section in Table A.1. Using the mentioned relay settings, the TMT index for examining the protection coordination conditions of relay pairs for all 68 defined scenarios is calculated and reported in Table 3.

Review of the results in Table 3 raises concern over the coordination conditions between the relay pairs. As mentioned in Section 4.1.2, TMT index is actually the sum of mis-coordination time values of incorrectly coordinated relay pairs for each scenario; hence the more negative the value, the worse the coordination of the relay pairs in the related scenario will be.

For instance, more than 30 scenarios have a TMT index less than −12 s where the worst scenario in this case is scenario 13 which has the minimum value of −13.95 s among others. The best scenario with the maximum TMT index value is scenario 1 with almost zero (0^-) seconds; this was guessable as the protection problem has been optimized for scenario 1 in the first phase.

Note that the total average value of TMT index for phase one is −6.6632 s; this gives a general overview on the coordination conditions between relay pairs for all scenarios. This value shows a weak protection coordination for the microgrid and its operation scenarios in general.

These results are not acceptable in any protection system because if the microgrid changes the operation mode into any of these incorrectly coordinated scenarios, then most of the fault currents will not be cleared coordinately as planned. Hence, applying a conventional protection scheme in this case study does not satisfy the protection coordination between the relay pairs.

For further investigation, the results of the average tripping time of the relays for each scenario are illustrated in Fig. 3. According to this figure, the maximum and minimum average tripping time of the relays in phase one belong to scenario 13 with 1.1 s and scenario 65 with 0.726 s respectively. The maximum value indicates the scenario with the worst operating time conditions, while the minimum value reveals the scenario with the best operating time conditions.

Also, to give a general overview on the operating time of the relays as a protection condition in the microgrid, the total average tripping time of the relays for the whole 68 scenarios is calculated and obtained as 0.8936 s. The results for min/max and total average indexes are almost normal considering the hugeness of the studied interconnected microgrid; meanwhile, execution of the second phase of the proposed scheme might bring even better results for this protection condition.

6.2. Phase two (Clustering Method)

In the next step, using previously gathered TDS and pick-up current settings of the relays in Table A.1, the MRPM with 68 columns (number of selected scenarios) and 100 rows (number of possible main/backup relay pairs) is formed as described in Section 4.1.3. The MRPM is used as an input data set to train SOM clustering algorithm.

The selected parameter settings for training of SOM algorithm are chosen based on suggestions in [36,45,46], with minor adjustments to optimize the clustering results. These parameters are presented in Table B.1 of Appendix B section.

Table 4
TMT index values for scenarios of each cluster (Phase 2).

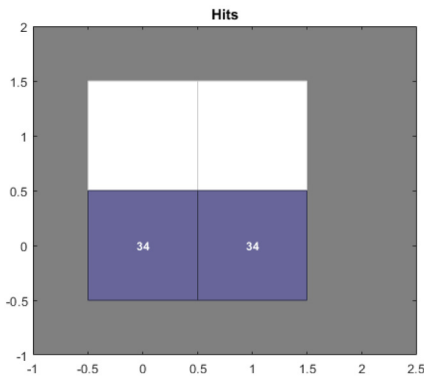| Cluster 1				Cluster 2			
Scenario	TMT (s)	Scenario	TMT (s)	Scenario	TMT (s)	Scenario	TMT (s)
65	−0.00032	35	−1.16369	13	−0.00038	20	−0.16662
1	−1.17235	36	−1.16321	2	−0.10223	37	−1.42624
4	−0.01593	53	−0.02014	3	−1.4402	38	−1.43353
21	−1.17758	54	−0.01785	5	−0.05896	39	−1.44669
22	−1.17489	55	−0.01408	6	−0.07892	40	−1.45276
23	−1.17017	56	−0.01283	7	−0.15318	41	−1.42067
24	−1.17117	57	−0.03574	8	−0.12798	42	−1.42842
25	−1.19085	58	−0.0255	9	−0.03558	43	−1.45607
26	−1.18061	59	−0.00807	10	−0.06088	44	−1.4709
27	−1.16593	60	−0.00565	11	−0.18255	45	−1.40411
28	−1.16166	61	−0.04018	12	−0.14248	46	−1.41267
29	−1.19621	62	−0.03785	14	−0.01254	47	−1.41219
30	−1.19346	63	−0.0298	15	−0.01475	48	−1.42065
31	−1.18598	64	−0.02752	16	−0.03273	49	−1.48273
32	−1.18322	66	−0.0026	17	−0.22479	50	−1.47699
33	−1.15947	67	−0.00463	18	−0.2025	51	−1.46822
34	−1.15896	68	−0.00604	19	−0.18966	52	−1.46234
Average TMT		**−0.5963 s**		**−0.7735 s**			

Fig. 4. SOM clustering hits map.

Since most of the digital overcurrent relays have 4 available setting groups, the output lattice size given to the SOM algorithm is considered as (2 × 2). Note that, Euclidean distance formula [24] is used to calculate the distance parameter in (9). The results for SOM algorithm hits map are displayed in Fig. 4.

As observed in Fig. 4, SOM divided 68 scenarios into 2 clusters, based on mis-coordinated relay pairs with each cluster including 34 scenarios equally.

Afterwards, the respective CMCMs are calculated for each cluster by the relay settings provided in Table A.1. Fig. 5 depicts the CMCM element values for cluster 1 and cluster 2. According to the description in Section 4.1.5, it seems in Fig. 5(a) that the scenario 65 has the minimum value and therefore is picked as the corresponding TMES for cluster 1. As with cluster 1, in Fig. 5(b) the scenario 13 is chosen as TMES for cluster 2.

Using genetic algorithm, the OF is minimized for each TMES with the related TDS and pick-up current settings being obtained for each relay. The relay settings are shown in Table A.2 and Table A.3 of Appendix A for cluster 1 and cluster 2, respectively.

Then, the TMT results are checked by applying the relay settings of Table A.2 and Table A.3 to each scenario of cluster 1 and cluster 2, respectively in Table 4.

Based on Table 4, it can be easily understood that the TMT index value for scenario 29 is −1.196 s which is the minimum in cluster 1 where scenario 49 has the same condition in cluster 2 by TMT value as −1.482 s. These scenarios have the worst coordination conditions between relay pairs of the microgrid among others.

Predictably, the best coordination conditions between relay pairs or the maximum TMT index value between other scenarios belongs to scenario 65 in cluster 1 with almost zero (0^-) seconds and scenario 13 in cluster 2 with almost the same condition (0^-). The protection coordination problem is optimized for these particular scenarios (TMESs) and therefore they claim the best protection coordination results.

Undeniably, the value of TMT index for each scenario in the second phase has improved significantly. For instance, the comparison of minimum TMT index value (worst condition) between phase 1 and phase 2 of the proposed algorithm shows almost 91.43% reduction for scenario 29 in cluster 1 and 89.38% reduction for scenario 49 in cluster 2 against scenario 13 in phase one with −13.95 s.

Comparing against −6.6632 s in the first phase, the size of the mean value of TMT index for cluster 1 is reduced by 6.06 s to −0.5963 s and also reduced by 5.88 s to −0.7735 s for cluster 2. It is visible that cluster 1 has slightly better TMT results against cluster 2.

For further studies, the results of the average tripping time of overcurrent relays for the fault exactly in front of the main relays in cluster 1 and cluster 2 are illustrated in Fig. 6. According to their analysis, the maximum average tripping time of the relays (the worst case) belongs to scenario 29 with 0.729 s for cluster 1 and scenario 13 with 0.856 s for cluster 2. Scenario 65 with 0.714 s and scenario 49 with 0.749 s have the minimum average tripping time of the relays for cluster 1 and cluster 2 respectively.

Also the total average value for the entire cluster 1 is 0.7213 s while 0.7983 s for cluster 2. Based on the results obtained from phase one, which is 0.8936 s, the average tripping time value for cluster 1 has diminished by 19.28% and by 10.66% for cluster 2, respectively. Again, it can be seen that cluster 1 has better results albeit non-significant.

Although all the facts describe the efficiency of the work, still existence of scenarios with TMT index less than −1 s does not guarantee the healthy protection of the microgrid; thus, since there are still two more empty clusters, i.e. two setting groups of the digital relays are yet to be used, employment of the third phase of the proposed algorithm seems vital.
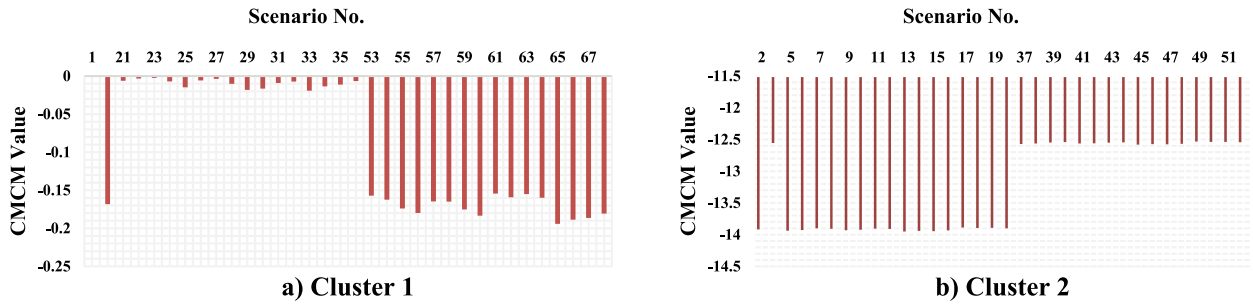
Fig. 5. The related CMCM element values of each cluster.
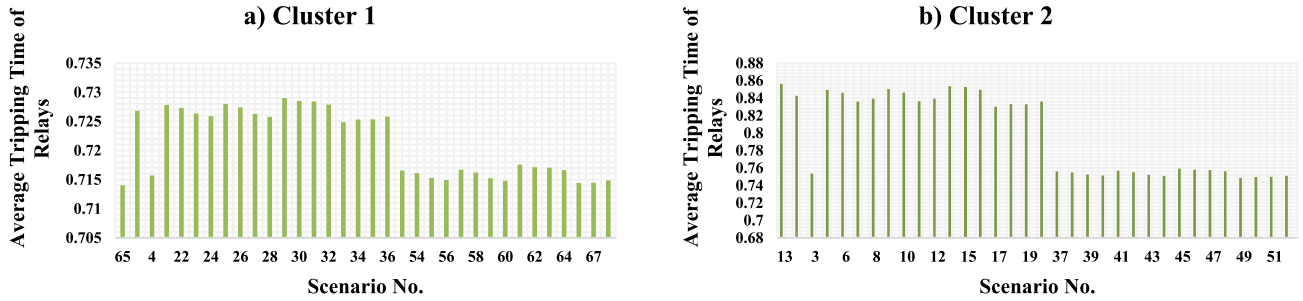
Fig. 6. Relays average tripping time for each scenario in the related cluster (phase 2).
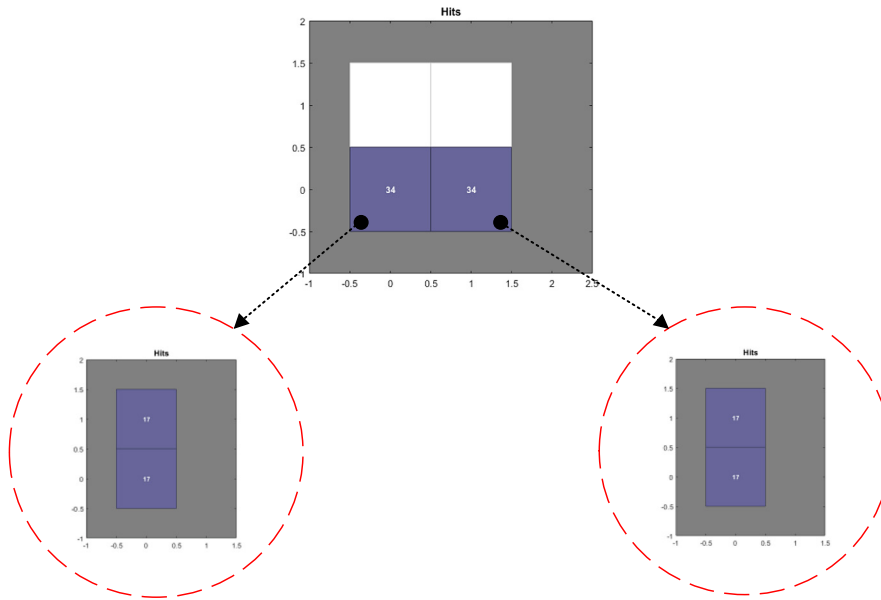
Fig. 7. SOM sub-clustering hits map for cluster 1 and 2.

6.3. Phase three (Sub-clustering Method)

Given the close results between cluster 1 and 2 in the second phase, both clusters are considered for the sub-clustering purpose. Hence, based on the description of Section 4.1.3, using relay settings of Tables A.2 and A.3, two MRPMs are formed, one for the set of cluster 1 scenarios and another for the set of cluster 2 scenarios, both with 34 columns (number of scenarios) and 100 rows.

MRPMs are used as an input data set for SOM training. Knowing the lattice size (2 × 1) dimensions for each selected cluster, SOM divides each one into two sub-clusters. The results of SOM algorithm hits maps are presented in Fig. 7.

Totally there are 4 sub-clusters once the SOM process is done with each including 17 scenarios. Sub-clusters 1.1 and 1.2 are gained from cluster 1 while sub-clusters 2.1 and 2.2 from cluster 2.

Note that the reason why the cluster members are all equal to 17 is because of the weak short circuit feeding capabilities of EV charging stations. Therefore, it seems that the SOM clustering is independent of the defined uncertainties of these DER units.

Afterwards, based on the relay settings of Table A.2, CMCM is created for sub-clusters 1.1 and 1.2, respectively; according to the relay settings of Table A.3, the related CMCM is calculated for sub-clusters 2.1 and 2.2. Meanwhile, the CMCM element values are presented in Fig. 8 for each sub-cluster.
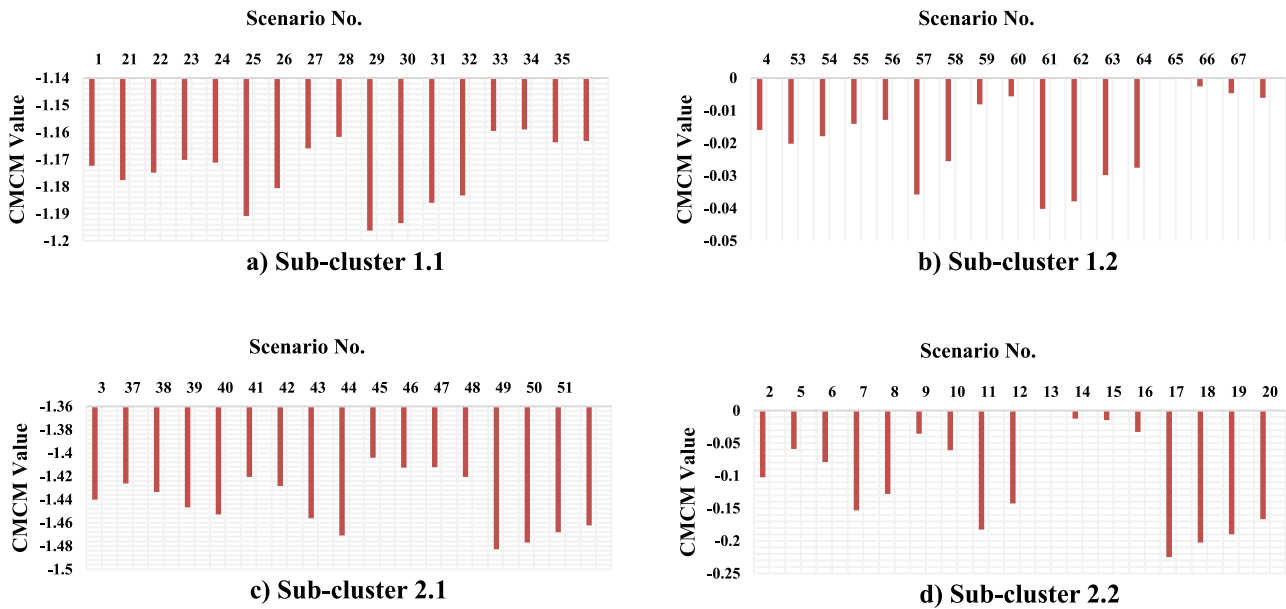
Fig. 8. The related CMCM element values of each Sub-cluster.

Following the procedure, TMES is determined by analyzing the related CMCM for each sub-cluster in Fig. 8 as follows:

(a) Scenario 29 for sub-cluster 1.1,
(b) Scenario 61 for sub-cluster 1.2,
(c) Scenario 49 for sub-cluster 2.1,
(d) Scenario 17 for sub-cluster 2.2.

OF is optimized for each TMES after which the obtained relay settings are stored in Tables A.4–A.7 for each sub-cluster. By applying these relay settings to their respective sub-clusters, the protection coordination conditions are checked. Final TMT index values are provided in Table 5 for each sub-cluster.

According to Table 5, the minimum TMT index value for sub-cluster 1.1 belongs to scenario 33 with −0.061 s and scenario 65 with −0.058 s for sub-cluster 1.2. Also, scenario 45 with −0.108 s and scenario 13 with −0.175 s have the minimum TMT index values in sub-cluster 2.1 and 2.2 respectively.

Expectedly, scenarios 29, 61, 49, and 17 (selected TMESs) with almost zero (0^-) seconds have the maximum TMT index value and the best protection coordination conditions of sub-cluster 1.1, 1.2, 2.1, and 2.2 respectively.

To understand how much the coordination conditions improve in the third phase of the proposed scheme, it should be pointed that the minimum TMT index value of sub-cluster 1.1 in comparison with cluster 1 is reduced by 94.9% and 95.15% for sub-cluster 1.2. Also the same comparison between sub-cluster 1.1 and conventional protection method shows 99.56% reduction and 99.58% for the same comparison of sub-cluster 1.2.

In the same way, the minimum TMT index value of sub-cluster 2.1 and 2.2 in comparison with cluster 2 in second phase is reduced by 92.71% for sub-cluster 2.1 and 88.19% for sub-cluster 2.2. The same comparison with the first phase minimum TMT shows 99.23% reduction for sub-cluster 2.1 and also 98.75% reduction for sub-cluster 2.2.

In addition, checking TMT index results in Table 5, brings an interesting quality of the work that was not predictable from the beginning; it is the fact that TMT index values for 61 scenarios are smaller than −0.1 s by the size, which is a great outcome suggesting that for these 61 operation scenarios, the selected relay settings will provide almost the perfect protection coordination.

Considering the fact that CTI value is selected 0.3 s in this project, even those 7 scenarios with TMT index values greater than −0.1 s by the size, will provide sufficient protection coordination between relay pairs. Thus, these results guarantee that the main/backup relay priority is always considered in this protection system, and so the protection system has adequate response to the fault occurrence.

Further, to give an overall overview on protection coordination conditions between relay pairs of each sub-cluster, the mean value of TMT index is calculated and given in Table 5. The results are −0.0266, −0.0263, −0.0493 and −0.08 s for sub-clusters 1.1, 1.2, 2.1, and 2.2 respectively.

In comparison with −6.6632 s in the phase one, the size of the average TMT index is reduced by more than 6.58 s for all sub-clusters. Also, as compared with −0.5963 s in cluster 1 of phase two, more than 0.56 s reduction for sub-clusters 1.1 and 1.2 is achieved. Further, in comparison with −0.7735 s in cluster 2 of phase two, the size of average TMT index is reduced more than 0.69 s for sub-clusters 2.1 and 2.2. The improvement of the mean value of TMT index is significant and undeniable.

For further examination, the average tripping time of the relays for the fault exactly in front of them is calculated in each sub-cluster with the results being illustrated in Fig. 9. Analysis of the mentioned figure indicates that scenario 29 with 0.742 s, scenario 61 with 0.716 s, scenario 45 with 0.725 and scenario 13 with 0.776 s have the maximum average tripping time and the worst protection condition among other scenarios in sub-clusters 1.1, 1.2, 2.1, and 2.2 respectively.

For the minimum average tripping time of the relays in each sub-cluster, it is found that scenario 33 with 0.737 s for sub-cluster 1.1, scenario 65 with 0.712 s for sub-cluster 1.2, scenario 49 with 0.719 s for sub-cluster 2.1 and scenario 17 with 0.768 s for sub-cluster 2.2 have the best protection condition among others.

It is observed that the distance between min/max scenarios in each sub-cluster become so close in comparison with the first two phases. Thus, the total average value for each sub-cluster gives a far better overview on this protection condition, with the values of the mentioned index being as follows:

(a) 0.7399 s for sub-cluster 1.1,
(b) 0.7145 s for sub-cluster 1.2,
(c) 0.7220 s for sub-cluster 2.1,
(d) 0.7727 s for sub-cluster 2.2.

Table 5
TMT index values for scenarios of each sub-cluster (phase 3).

Cluster 1				Cluster 2			
Sub-cluster 1.1		Sub-cluster 1.2		Sub-cluster 2.1		Sub-cluster 2.2	
Scenario	TMT (s)	Scenario	TMT (s)	Scenario	TMT (s)	Scenario	TMT (s)
29	−0.00113	61	−0.00023	49	−0.00068	17	−0.00044
1	−0.02296	4	−0.02389	3	−0.04439	2	−0.07164
21	−0.01107	53	−0.01464	37	−0.07621	5	−0.12723
22	−0.01567	54	−0.01834	38	−0.05991	6	−0.09901
23	−0.0318	55	−0.03099	39	−0.03147	7	−0.03675
24	−0.0406	56	−0.03827	40	−0.025	8	−0.04705
25	−0.01107	57	−0.00998	41	−0.08146	9	−0.12832
26	−0.01434	58	−0.01463	42	−0.0598	10	−0.09547
27	−0.0339	59	−0.03384	43	−0.0306	11	−0.04461
28	−0.04474	60	−0.04383	44	−0.02603	12	−0.05233
30	−0.00481	62	−0.00428	45	−0.10889	13	−0.17547
31	−0.00475	63	−0.0061	46	−0.09233	14	−0.14872
32	−0.00796	64	−0.00962	47	−0.09167	15	−0.1498
33	−0.06148	65	−0.0583	48	−0.07533	16	−0.12218
34	−0.05283	66	−0.05086	50	−0.01005	18	−0.01932
35	−0.05125	67	−0.04836	51	−0.00795	19	−0.01344
36	−0.04246	68	−0.04097	52	−0.0165	20	−0.02937
Average TMT	**−0.0266 s**	**−0.0263 s**		**−0.0493 s**		**−0.0800 s**	
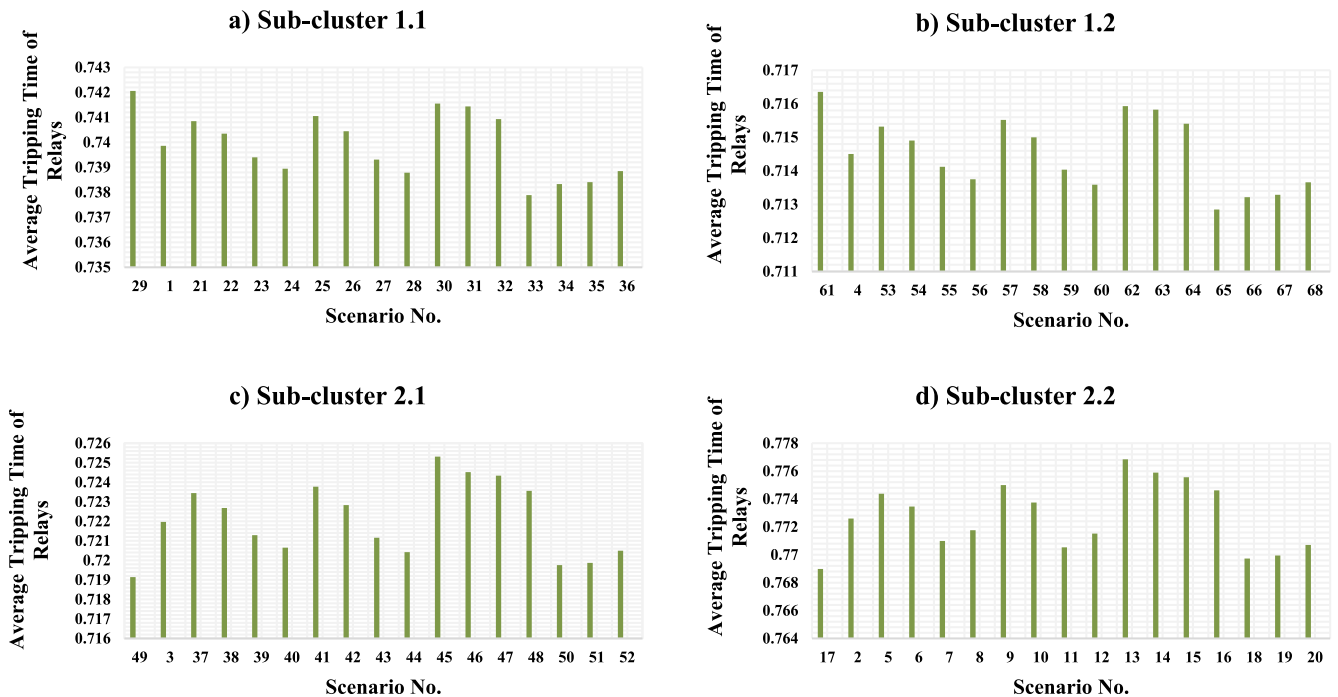
Fig. 9. Relays average tripping time for each scenario in the respective sub-cluster.

The total average tripping time value for sub-cluster 1.1 shows 2.57% increase and 17.2% reduction in comparison with cluster 1 and conventional protection scheme. The same index for sub-cluster 1.2 indicates 0.94% and 20.04% reduction in comparison with cluster 1 in phase 2 and conventional protection scheme in phase 1 respectively.

This index results for sub-cluster 2.1 shows 9.55% and 19.2% reduction in comparison with cluster 2 and first phase results. Also for sub-cluster 2.2, 3.2% and 13.53% reduction are visible in the same comparison.

Totally, considering all the facts, the operating time of overcurrent relays as a protection condition are also in a better status.

6.4. K-means clustering algorithm

In order to compare SOM clustering algorithm with other non-SOM and conventional clustering techniques, k-means clustering method is chosen.

K-means or Lloyd's algorithm [47] is one the most famous clustering methods that has frequently been used in different researches so far. The k-means algorithm is simple:

First step – The set of data points for clustering, the number of clusters and the maximum iteration number is specified.

Second step – Initial cluster centers are determined.

Third step – Based on the nearest distance between each data point and cluster centers, cluster members are selected.

Table 6
TMT index values for scenarios of each cluster (k-means method).

Cluster 1				Cluster 2		Cluster 3		Cluster 4	
Scenario	TMT	Scenario	TMT	Scenario	TMT	Scenario	TMT	Scenario	TMT
65	−0.00032	35	−1.16369	2	−0.00043	17	−0.00044	44	−0.00032
1	−1.17235	36	−1.16321	38	−0.00592	2	−0.07164	36	−0.05321
4	−0.01593	53	−0.02014	39	−0.01975	5	−0.12723	37	−0.07084
21	−1.17758	54	−0.01785	42	−0.01187	6	−0.09901	40	−0.02708
22	−1.17489	55	−0.01408	43	−0.03688	7	−0.03675	41	−0.05718
23	−1.17017	56	−0.01283	48	−0.05801	8	−0.04705	45	−0.0067
24	−1.17117	57	−0.03574	49	−0.04499	9	−0.12832	46	−0.01702
25	−1.19085	58	−0.0255	50	−0.03684	10	−0.09547	47	−0.03361
26	−1.18061	59	−0.00807	51	−0.02132	11	−0.04461		
27	−1.16593	60	−0.00565			12	−0.05233		
28	−1.16166	61	−0.04018			13	−0.17547		
29	−1.19621	62	−0.03785			14	−0.14872		
30	−1.19346	63	−0.0298			15	−0.1498		
31	−1.18598	64	−0.02752			16	−0.12218		
32	−1.18322	66	−0.0026			18	−0.01932		
33	−1.15947	67	−0.00463			19	−0.01344		
34	−1.15896	68	−0.00604			20	−0.02937		
Average TMT		**−0.5963 s**		**−0.0262 s**		**−0.0800 s**		**−0.0333 s**	
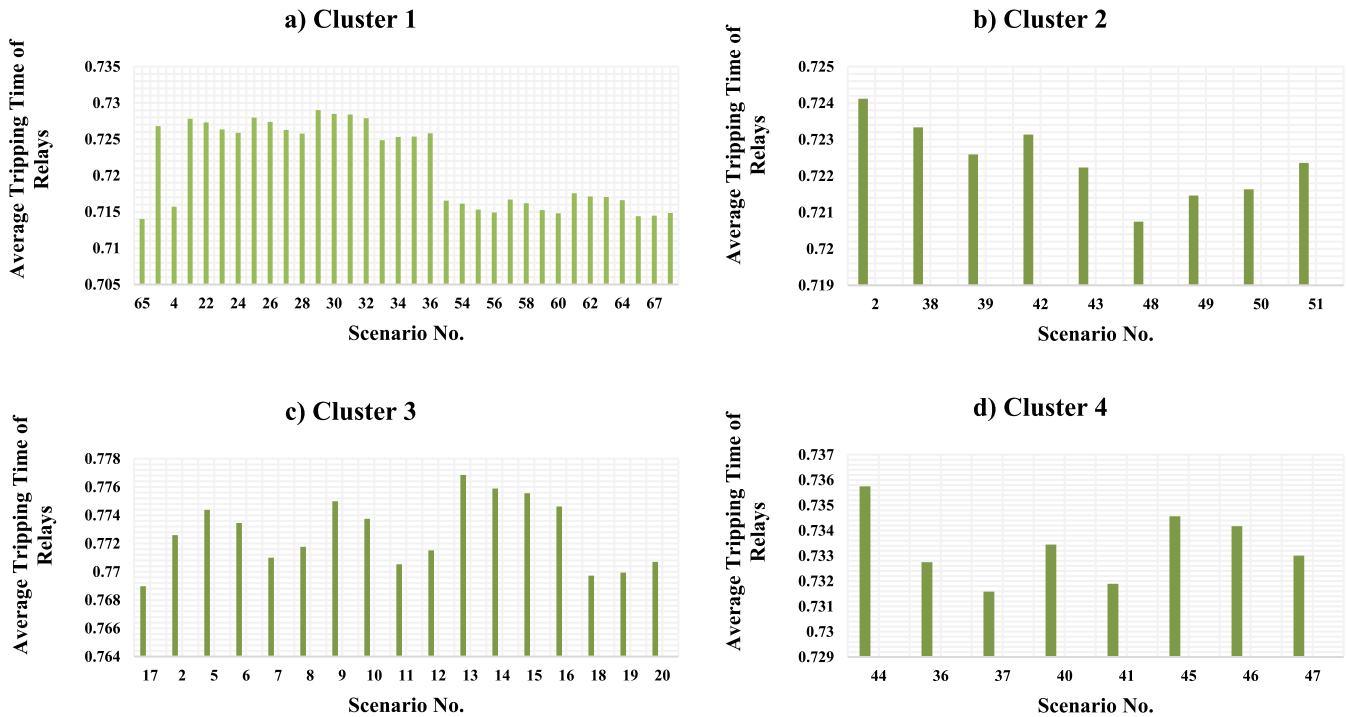
Fig. 10. Relays average tripping time for the scenarios of each cluster (k-means method).

Fourth step – The average value of the data points in each cluster is calculated and then replaced with the respected cluster center.

Fifth step – The algorithm repeats from the third step as long as the newly calculated cluster centers are different from their older values or the maximum iteration number is not reached; otherwise the clustering process is done.

To achieve comparable results between SOM and k-means clustering algorithm, the proposed method in Section 4 is repeated again by replacing k-means algorithm with SOM method. Further, for supporting k-means algorithm to make more competitive results against SOM, k-means++ algorithm [48] is implemented in this research.

The first phase of the proposed protection scheme is same for both clustering methods; hence, this section starts by implementation of the second phase. The input data points for k-means clustering are selected as same as the input data created in step 3 of phase 2 of the proposed method as MRPM. The number of clusters is defined as equal to the number of setting groups of digital overcurrent relays, which is considered 4 in this paper.

The k-means algorithm is executed and divides 68 scenarios into 4 clusters with 34, 9, 17, and 8 scenarios. Meanwhile, it is found that the third phase (sub-clustering) cannot be executed this time. In the next step, using relay settings in Table A.1, the related CMCM is created for each cluster after which by analyzing

Table 7
The final summary.

	Phase I	Phase II	Phase III	k-Means
Applied protection and methods	Conventional protection scheme (non-adaptive method)	Proposed adaptive protection scheme (SOM clustering method)	Proposed adaptive protection scheme (SOM sub-clustering method)	Proposed adaptive protection scheme (k-Means based method)
Total average value of TMT index (s)	−6.6632	−0.6849	−0.0456	−0.3255
Total average tripping time of the relays (s)	0.8936	0.7598	0.7373	0.7357

Table A.1
Relay settings for conventional protection scheme (Base Scenario).

Relay	TDS	Pick-up	Relay	TDS	Pick-up	Relay	TDS	Pick-up	Relay	TDS	Pick-up
1	1.184	187.5	20	0.209	50	39	0.051	150	58	0.051	37.5
2	1.014	150	21	0.695	37.5	40	0.199	50	59	0.051	75
3	0.803	50	22	0.999	75	41	0.344	50	60	0.147	75
4	0.588	50	23	0.807	75	42	0.498	50	61	0.292	56.25
5	0.389	50	24	0.699	56.25	43	0.614	50	62	0.051	56.25
6	0.231	50	25	1.057	56.25	44	0.696	75	63	0.168	56.25
7	0.051	75	26	0.87	56.25	45	0.051	100	64	0.291	56.25
8	0.051	100	27	0.691	56.25	46	0.051	37.5	65	0.49	37.5
9	0.691	37.5	28	0.603	37.5	47	0.216	37.5	66	0.051	56.25
10	0.518	37.5	29	1.021	56.25	48	0.386	37.5	67	0.21	25
11	0.349	37.5	30	1.056	25	49	0.071	15	68	0.317	37.5
12	0.449	15	31	0.783	37.5	50	0.306	15	69	0.453	37.5
13	0.247	15	32	0.623	37.5	51	0.633	25	70	0.051	25
14	0.051	25	33	0.564	25	52	0.051	50	71	0.051	50
15	0.986	50	34	1.061	50	53	0.182	37.5	72	0.514	37.5
16	0.892	37.5	35	0.209	37.5	54	0.322	37.5	73	0.469	37.5
17	0.739	37.5	36	0.593	37.5	55	0.051	50	74	0.49	37.5
18	0.746	50	37	0.608	37.5	56	0.179	50			
19	0.389	50	38	0.051	187.5	57	0.343	50			

them, TMES is chosen for each one. Based on the ordered instructions in Sections 4.1.5 and 4.2.2, scenario 65, scenario 35, scenario 17, and scenario 44 are selected as TMES for clusters 1, 2, 3, and 4 respectively.

Then, the optimized relay settings are calculated for each TMES and applied to the scenarios of the related cluster. The TDS and pick-up current settings for cluster 2 and cluster 4 are presented in Appendix A section as Table A.8 and Table A.9 respectively. Note that the clustering results for cluster 1 and 3 completely match earlier SOM results as cluster 1 in phase two and sub-cluster 2.2 in phase 3 respectively. Thus, their related relay settings are the same as provided in Tables A.2 and A.7 of Appendix A.

Afterwards, protection coordination conditions between relay pairs is checked as TMT index value for scenarios of each cluster. The final results of k-means clustering and TMT index values are given in Table 6.

Examination of Table 6 indicates that scenario 29 with −1.196 s, scenario 48 with −0.058 s, scenario 13 with −0.175 s and scenario 37 with −0.07 s have the minimum TMT index values (the worst scenarios) among others.

Comparing minimum TMT results of k-means method with SOM method in the third phase indicates weakness of k-means based method in this case study. In the third phase of the proposed scheme, none of the scenarios had TMT index values less than −0.175 s which almost guarantees the healthy protection coordination conditions between relay pairs and which is in line with the priority of main/backup relay pairs in clearing fault currents.
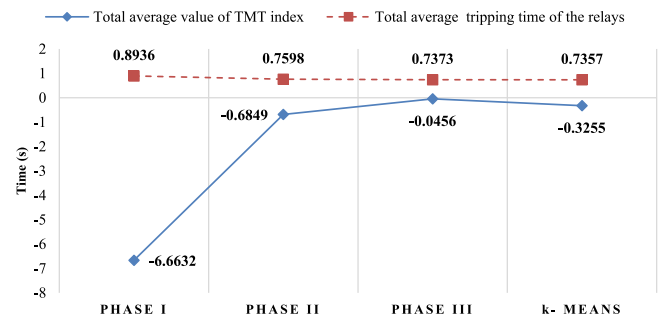
Fig. 11. Total average indices of each phase and k-means based method.

Conversely, in k-means based method, there are 17 scenarios with TMT index values less than −1.1 s, which is not acceptable for protection system and there might be extensive fault currents in the microgrid that are not cleared coordinately by the main/backup relay pairs.

For further investigation, the average TMT index values are also provided in Table 6. Again, their investigation indicates the weakness of k-means based method against the proposed scheme, where the worst (minimum) average TMT index in the third phase of the proposed scheme was −0.08 s for sub-cluster 2.2, while in k-means based method it is −0.596 s which is a substantial difference in protection systems.

Also, the results for the average tripping time of the relays in each scenario are shown in Fig. 10. Analyzing the figure shows

Table A.2
The relay settings for TMES of cluster 1.

Relay	TDS	Pick-up	Relay	TDS	Pick-up	Relay	TDS	Pick-up	Relay	TDS	Pick-up
1	1.037	312.5	20	0.154	150	39	0.051	187.5	58	0.051	75
2	0.948	187.5	21	0.57	75	40	0.145	125	59	0.051	75
3	0.622	125	22	0.99	75	41	0.252	125	60	0.151	75
4	0.449	125	23	0.797	75	42	0.368	125	61	0.269	75
5	0.292	125	24	0.635	75	43	0.449	125	62	0.051	37.5
6	0.176	125	25	1.186	37.5	44	0.68	75	63	0.189	37.5
7	0.051	75	26	0.978	37.5	45	0.051	150	64	0.333	37.5
8	0.051	150	27	0.778	37.5	46	0.051	56.25	65	0.553	25
9	0.632	56.25	28	0.67	25	47	0.201	56.25	66	0.051	93.75
10	0.474	56.25	29	0.866	93.75	48	0.356	56.25	67	0.201	37.5
11	0.32	56.25	30	0.948	37.5	49	0.051	37.5	68	0.337	37.5
12	0.364	37.5	31	0.782	37.5	50	0.215	37.5	69	0.477	37.5
13	0.203	37.5	32	0.621	37.5	51	0.364	50	70	0.051	62.5
14	0.051	50	33	0.446	62.5	52	0.051	50	71	0.051	50
15	1.007	50	34	0.483	50	53	0.157	56.25	72	0.419	75
16	0.811	56.25	35	0.182	75	54	0.28	56.25	73	0.41	56.25
17	0.672	56.25	36	0.541	56.25	55	0.051	125	74	0.4	75
18	0.607	125	37	0.492	75	56	0.142	125			
19	0.302	125	38	0.051	312.5	57	0.25	150			

Table A.3
The relay settings for TMES of cluster 2.

Relay	TDS	Pick-up	Relay	TDS	Pick-up	Relay	TDS	Pick-up	Relay	TDS	Pick-up
1	0.05	125	20	0.051	75	39	0.282	75	58	0.359	75
2	0.252	75	21	0.163	75	40	0.392	50	59	0.051	75
3	0.254	50	22	0.318	75	41	0.501	50	60	0.108	75
4	0.148	50	23	0.213	75	42	0.617	50	61	0.259	37.5
5	0.051	50	24	0.161	37.5	43	0.477	125	62	0.051	75
6	0.263	125	25	0.406	75	44	0.419	225	63	0.091	75
7	0.051	225	26	0.252	75	45	0.405	250	64	0.141	75
8	0.051	250	27	0.141	75	46	0.051	93.75	65	0.241	62.5
9	0.665	93.75	28	0.051	62.5	47	0.116	93.75	66	0.051	56.25
10	0.561	93.75	29	0.673	56.25	48	0.188	93.75	67	0.143	50
11	0.46	93.75	30	0.578	50	49	0.051	15	68	0.228	56.25
12	0.584	15	31	0.45	56.25	50	0.256	15	69	0.28	75
13	0.409	15	32	0.307	75	51	0.548	25	70	0.481	25
14	0.219	25	33	0.548	25	52	0.051	100	71	0.051	125
15	0.588	100	34	0.571	125	53	0.085	93.75	72	0.051	75
16	0.497	93.75	35	0.461	75	54	0.138	93.75	73	0.2	93.75
17	0.408	93.75	36	0.325	93.75	55	0.338	75	74	0.38	37.5
18	0.19	75	37	0.051	37.5	56	0.427	75			
19	0.102	75	38	0.051	125	57	0.541	75			

that the maximum average tripping time of the relays (the worst condition) belongs to scenario 29 with 0.729 s, scenario 2 with 0.724 s, scenario 13 with 0.776 s and scenario 44 with 0.735 s in cluster 1, 2, 3 and 4 respectively. The maximum average tripping time among all scenarios for SOM based method in the third phase was 0.776 s which is the same as k-means based results.

Further, scenario 65 with 0.714 s in cluster 1, scenario 48 with 0.72 s in cluster 2, scenario 17 with 0.768 s in cluster 3 and scenario 37 with 0.731 s in cluster 4 have the minimum average tripping time of the relays. The minimum average tripping time among all scenarios for SOM based method in third phase was 0.712 s which is slightly better than 0.714 s in k-means based method.

For more comparison, the total average tripping time for each cluster is calculated as follows:

(a) 0.7213 s for cluster 1,
(b) 0.7224 s for cluster 2,
(c) 0.7727 s for cluster 3,
(d) 0.7334 s for cluster 4.

Since the number of members of each cluster in k-means based method is not equal, thus the average tripping time calculated for each cluster does not show the same weight as others; thus, for comparison of k-means and SOM based methods, total weight average value is calculated for both methods.

The total weight average of tripping time of the relays in k-means based method is 0.7357 s and the same for SOM based method in the third phase is 0.7373 s. It is found that k-means based method has 0.0016 s better result.

The k-means based method is executed with the final results being provided and discussed completely. It seems that SOM based method a significant advantage over k-means based method when comparing the TMT index values as an important protection coordination condition. Comparing the average tripping time of the relays, the results were almost equal but slightly in favor of k-means based method. Considering all the facts, it

Table A.4
The relay settings for TMES of sub-cluster 1.1.

Relay	TDS	Pick-up	Relay	TDS	Pick-up	Relay	TDS	Pick-up	Relay	TDS	Pick-up
1	1.01	312.5	20	0.213	50	39	0.051	225	58	0.051	37.5
2	0.881	225	21	0.694	37.5	40	0.163	100	59	0.051	125
3	0.679	100	22	0.855	125	41	0.307	75	60	0.131	112.5
4	0.533	75	23	0.706	112.5	42	0.442	75	61	0.27	75
5	0.353	75	24	0.637	75	43	0.61	50	62	0.051	75
6	0.238	50	25	0.979	75	44	0.61	112.5	63	0.174	56.25
7	0.051	112.5	26	0.868	56.25	45	0.051	100	64	0.296	56.25
8	0.051	100	27	0.689	56.25	46	0.051	37.5	65	0.454	50
9	0.691	37.5	28	0.555	50	47	0.216	37.5	66	0.051	93.75
10	0.518	37.5	29	0.873	93.75	48	0.386	37.5	67	0.232	25
11	0.349	37.5	30	1.052	25	49	0.068	15	68	0.336	37.5
12	0.448	15	31	0.78	37.5	50	0.301	15	69	0.472	37.5
13	0.246	15	32	0.622	37.5	51	0.624	25	70	0.051	37.5
14	0.051	25	33	0.508	37.5	52	0.051	75	71	0.051	75
15	0.869	75	34	0.927	75	53	0.164	56.25	72	0.513	37.5
16	0.793	56.25	35	0.209	37.5	54	0.284	56.25	73	0.412	56.25
17	0.658	56.25	36	0.531	56.25	55	0.051	75	74	0.438	56.25
18	0.666	75	37	0.54	56.25	56	0.16	75			
19	0.352	75	38	0.051	312.5	57	0.344	50			

Table A.5
The relay settings for TMES of sub-cluster 1.2.

Relay	TDS	Pick-up	Relay	TDS	Pick-up	Relay	TDS	Pick-up	Relay	TDS	Pick-up
1	1.088	250	20	0.209	50	39	0.051	187.5	58	0.051	37.5
2	0.943	187.5	21	0.691	37.5	40	0.18	75	59	0.051	100
3	0.736	75	22	0.922	100	41	0.308	75	60	0.14	93.75
4	0.54	75	23	0.755	93.75	42	0.506	50	61	0.299	56.25
5	0.397	50	24	0.697	56.25	43	0.624	50	62	0.051	56.25
6	0.239	50	25	1.064	56.25	44	0.626	112.5	63	0.169	56.25
7	0.051	112.5	26	0.876	56.25	45	0.051	150	64	0.293	56.25
8	0.051	150	27	0.696	56.25	46	0.051	37.5	65	0.452	50
9	0.7	37.5	28	0.56	50	47	0.219	37.5	66	0.051	75
10	0.524	37.5	29	0.923	75	48	0.392	37.5	67	0.196	37.5
11	0.352	37.5	30	0.934	37.5	49	0.051	22.5	68	0.287	56.25
12	0.413	22.5	31	0.682	56.25	50	0.221	30	69	0.408	56.25
13	0.212	30	32	0.541	56.25	51	0.387	37.5	70	0.051	25
14	0.051	37.5	33	0.571	25	52	0.051	75	71	0.051	50
15	0.872	75	34	0.48	50	53	0.144	75	72	0.456	56.25
16	0.722	75	35	0.189	56.25	54	0.252	75	73	0.367	75
17	0.596	75	36	0.478	75	55	0.051	50	74	0.499	37.5
18	0.734	50	37	0.606	37.5	56	0.183	50			
19	0.389	50	38	0.051	250	57	0.35	50			

seems that SOM based method has an overall and fair advantage over k-means based method.

6.5. Discussion

Finally, a summary of achieved results in all three phases of the proposed adaptive protection scheme and k-means based method is provided in Table 7. It gives a brief general overview for comparison between the non-adaptive method, proposed adaptive method and the k-means based method.

As can be seen in Table 7, the first row of the table defines the applied protection schemes and methods of the paper. The second row is presented in order to show the total average value of TMT index for all 68 defined scenarios in each method for comparison purposes. In this paper, the TMT index is selected as a representative of protection coordination conditions between relay pairs.

The third row is created in order to compare the results of the total average tripping time of the relays for all 68 defined scenarios in each method. In this research, the average tripping time of the relays has been chosen as a representative of operating time of the relays which is also a protection condition.

As mentioned earlier in Section 6.1, the total average value of TMT index in the first phase of the proposed scheme or so called conventional protection scheme is −6.6632 s; after executing second phase of the method, this value improved by 89.72% reduction to −0.6849 s. Finally, the mentioned index value is reduced even more by 93.34% comparing against the second phase result and become −0.0456 s which almost guarantees the perfect possible coordination between relay pairs of microgrid for each defined operation scenario.

Comparison between total average value of TMT index between k-means based method and the third phase of the proposed method reveals superiority of the proposed method by adopting SOM clustering approach against k-means clustering algorithm. The mentioned index value is −0.0456 s for the third

Table A.6
The relay settings for TMES of sub-cluster 2.1.

Relay	TDS	Pick-up	Relay	TDS	Pick-up	Relay	TDS	Pick-up	Relay	TDS	Pick-up
1	0.05	125	20	0.051	50	39	0.315	75	58	0.281	37.5
2	0.274	75	21	0.224	37.5	40	0.431	50	59	0.051	50
3	0.273	50	22	0.406	50	41	0.55	50	60	0.158	37.5
4	0.158	50	23	0.301	37.5	42	0.676	50	61	0.275	37.5
5	0.051	50	24	0.169	37.5	43	0.666	75	62	0.051	37.5
6	0.12	75	25	0.496	37.5	44	0.785	75	63	0.136	37.5
7	0.051	75	26	0.336	37.5	45	0.754	100	64	0.23	37.5
8	0.051	100	27	0.184	37.5	46	0.051	37.5	65	0.35	37.5
9	0.817	37.5	28	0.051	37.5	47	0.175	37.5	66	0.051	56.25
10	0.664	37.5	29	0.736	56.25	48	0.305	37.5	67	0.198	25
11	0.515	37.5	30	0.817	25	49	0.051	22.5	68	0.292	37.5
12	0.347	22.5	31	0.586	37.5	50	0.2	30	69	0.416	37.5
13	0.178	30	32	0.462	37.5	51	0.344	37.5	70	0.197	25
14	0.051	37.5	33	0.556	25	52	0.051	50	71	0.051	75
15	0.883	50	34	0.051	75	53	0.107	56.25	72	0.064	37.5
16	0.708	56.25	35	0.424	37.5	54	0.193	56.25	73	0.343	37.5
17	0.585	56.25	36	0.544	37.5	55	0.439	50	74	0.407	37.5
18	0.25	50	37	0.051	37.5	56	0.553	50			
19	0.133	50	38	0.051	125	57	0.694	50			

Table A.7
The relay settings for TMES of sub-cluster 2.2.

Relay	TDS	Pick-up	Relay	TDS	Pick-up	Relay	TDS	Pick-up	Relay	TDS	Pick-up
1	0.05	125	20	0.051	50	39	0.289	75	58	0.263	37.5
2	0.251	75	21	0.206	37.5	40	0.399	50	59	0.051	50
3	0.256	50	22	0.384	50	41	0.51	50	60	0.15	37.5
4	0.149	50	23	0.287	37.5	42	0.628	50	61	0.259	37.5
5	0.051	50	24	0.162	37.5	43	0.543	100	62	0.051	56.25
6	0.083	100	25	0.41	56.25	44	0.72	75	63	0.141	37.5
7	0.051	75	26	0.321	37.5	45	0.69	100	64	0.224	37.5
8	0.051	100	27	0.177	37.5	46	0.051	56.25	65	0.335	37.5
9	0.679	56.25	28	0.051	37.5	47	0.17	37.5	66	0.051	56.25
10	0.633	37.5	29	0.707	56.25	48	0.285	37.5	67	0.188	25
11	0.491	37.5	30	0.799	25	49	0.064	15	68	0.27	37.5
12	0.513	15	31	0.572	37.5	50	0.264	15	69	0.383	37.5
13	0.348	15	32	0.454	37.5	51	0.534	25	70	0.191	25
14	0.167	25	33	0.519	25	52	0.051	50	71	0.051	50
15	0.822	50	34	0.89	50	53	0.135	37.5	72	0.057	37.5
16	0.754	37.5	35	0.396	37.5	54	0.234	37.5	73	0.341	37.5
17	0.624	37.5	36	0.501	37.5	55	0.408	50	74	0.382	37.5
18	0.233	50	37	0.051	37.5	56	0.515	50			
19	0.124	50	38	0.051	125	57	0.647	50			

phase of the proposed method, while the same value for k-means based approach is −0.3255 s which is increased by 0.28 s.

The total average tripping time of the relays for conventional protection scheme is calculated as 0.8936 s; by implementing the second phase of the proposed adaptive method it is decreased by 14.97% to 0.7598 s. Then, in comparison of the second phase, execution of the third phase of the proposed scheme reduced the mentioned index by 2.96% to 0.7373 s eventually. Although the reduction and improvement in this protection condition is not comparable with the other index, considering the fact that the studied microgrid has large series of power network, the resultant seems acceptable.

Comparing k-means based method result against SOM based approach indicates that k-means based method has a slight advantage in the total average tripping time index. K-means based method as mentioned in Section 6.4 is 0.7357 s which is 0.0016 s better than SOM base method with 0.7373 s.

In order to highlight the improvement in the final results, the total average value TMT index and total average tripping time of the relays already presented in Table 7, are shown in Fig. 11 for each phase and k-means based method, respectively.

The discussed adaptive protection scheme is robust and effectively flexible to solve the similar protection problems in any power network in which the protection system is based on digital overcurrent relays.

Some of the key features which make the proposed scheme effective to other similar problems are as follows:

- The OF employed in this paper has the ability to simultaneously optimize the operating time of the relays and coordination time between main/backup relay pairs. This feature gives the advantage of examination of both protection conditions in this paper unlike other similar works. Similar approaches usually do not consider both conditions for optimization and mostly fail to improve the quality of the results in comparison with conventional protection scheme.
- The proposed TMT index, has the ability to evaluate the protection coordination between extensive numbers of the

Table A.8
The relay settings for TMES of cluster 2 (K-means Method).

Relay	TDS	Pick-up	Relay	TDS	Pick-up	Relay	TDS	Pick-up	Relay	TDS	Pick-up
1	0.05	125	20	0.051	75	39	0.323	75	58	0.261	56.25
2	0.275	75	21	0.191	56.25	40	0.439	50	59	0.051	50
3	0.272	50	22	0.4	50	41	0.557	50	60	0.128	56.25
4	0.157	50	23	0.257	56.25	42	0.682	50	61	0.268	37.5
5	0.051	50	24	0.168	37.5	43	0.595	100	62	0.051	56.25
6	0.113	100	25	0.439	56.25	44	0.673	112.5	63	0.117	56.25
7	0.051	112.5	26	0.294	56.25	45	0.628	150	64	0.239	37.5
8	0.051	150	27	0.184	37.5	46	0.051	56.25	65	0.358	37.5
9	0.729	56.25	28	0.051	37.5	47	0.184	37.5	66	0.051	37.5
10	0.676	37.5	29	0.834	37.5	48	0.314	37.5	67	0.161	37.5
11	0.527	37.5	30	0.697	37.5	49	0.051	30	68	0.239	56.25
12	0.317	30	31	0.488	56.25	50	0.204	30	69	0.345	56.25
13	0.178	30	32	0.384	56.25	51	0.347	37.5	70	0.227	25
14	0.051	37.5	33	0.549	25	52	0.051	75	71	0.051	50
15	0.744	75	34	0.051	50	53	0.096	75	72	0.054	56.25
16	0.614	75	35	0.386	56.25	54	0.168	75	73	0.248	75
17	0.504	75	36	0.401	75	55	0.44	50	74	0.398	37.5
18	0.262	50	37	0.051	37.5	56	0.555	50			
19	0.146	50	38	0.051	125	57	0.604	75			

Table A.9
The relay settings for TMES of cluster 4 (K-means Method).

Relay	TDS	Pick-up	Relay	TDS	Pick-up	Relay	TDS	Pick-up	Relay	TDS	Pick-up
1	0.05	125	20	0.051	75	39	0.309	75	58	0.285	75
2	0.275	75	21	0.167	75	40	0.424	50	59	0.051	75
3	0.271	50	22	0.343	75	41	0.541	50	60	0.14	56.25
4	0.157	50	23	0.257	56.25	42	0.665	50	61	0.282	37.5
5	0.051	50	24	0.168	37.5	43	0.582	100	62	0.051	75
6	0.161	100	25	0.392	75	44	0.526	187.5	63	0.103	75
7	0.051	187.5	26	0.266	75	45	0.466	250	64	0.198	56.25
8	0.051	250	27	0.163	56.25	46	0.051	75	65	0.314	50
9	0.694	75	28	0.051	50	47	0.143	75	66	0.051	37.5
10	0.572	75	29	0.796	37.5	48	0.273	56.25	67	0.129	62.5
11	0.504	56.25	30	0.539	62.5	49	0.051	30	68	0.208	75
12	0.332	30	31	0.403	75	50	0.204	30	69	0.269	93.75
13	0.178	30	32	0.279	93.75	51	0.347	37.5	70	0.319	25
14	0.051	37.5	33	0.534	25	52	0.051	100	71	0.051	50
15	0.645	100	34	0.051	50	53	0.067	112.5	72	0.051	75
16	0.504	112.5	35	0.397	75	54	0.137	93.75	73	0.205	93.75
17	0.449	93.75	36	0.356	93.75	55	0.368	75	74	0.411	37.5
18	0.209	75	37	0.051	37.5	56	0.464	75			
19	0.112	75	38	0.051	125	57	0.586	75			

relay pairs in a power network; thus, in similar projects with similar massive results to be analyzed, it is completely useful feature.

- The clustering procedure in this paper is based on mis-coordination between relay pairs of each scenario; thus, the clustering is not dependable on network topology and is executable on any different power network.
- Three phase clustering approach based on loser neurons in SOM clustering procedure ensures the perfect quality in protection conditions of the power network.
- The decentralized communication approach in this research allows this method to be implemented in any power network system because of the availability and existence of these communications between substations. Thus, this feature makes the protection scheme cost efficient. The only limitation of this feature is the number of available setting groups of these relays and therefore available clusters for clustering. This might make some challenges to the proposed scheme when facing power networks with so many

different operation scenarios. Nevertheless, either way the improvement of protection results is almost guaranteed.

Note that in any case, it is always possible to take a centralized communication approach as mentioned in Section 1 in order to achieve the most reliable results for protection conditions of the power network.

7. Conclusion

In this paper, for microgrids and power networks suffering from different short-circuit current levels due to different operation scenarios, DG's intermittency and uncertainties, a novel adaptive protection scheme has been introduced. The method has been described in three phases which employed SOM clustering technique, and is dependent on the use of digital overcurrent relays and their setting groups. Scenarios that are similar in mis-coordination between main/backup relay pairs have been divided into several clusters in phase 2 and several sub-clusters in phase 3; then for each (sub-)cluster, TMES has been selected

Table B.1
Parameter settings for SOM training.

Parameter	Value
Size	4
Dimensionality	2
Lattice topology	rectangular
Distance function	Euclidean
Number of epochs	200
Initial neighborhood size	3
Number of steps for initial covering of input space	100

among other scenarios by analyzing the respected CMCM. Afterwards, relay settings have been optimized for each TMES and hence applied to all scenarios in the respected (sub-)cluster. The protection coordination conditions of each phase have been analyzed, discussed and compared completely. As shown in the final results, the TMT index has been improved as a protection coordination condition between the main/backup relay pairs. However, it has not been comparable with TMT index, but the final outcome for average tripping time of the relays has been reduced and improved as well. Here, it is important to note that, the basis and first goal of the proposed protection scheme was to reduce the magnitude of mis-coordination intervals between the relay pairs and it has been successful in this matter completely. This is the reason why clustering input data set is based on mis-coordination data. Also, the final results of the proposed SOM clustering method have been compared against k-means method which indicated the advantage of the proposed SOM based method. At the end, it is concluded that the mentioned method is comprehensive, cost-efficient, flexible, and easy enough to handle the protection criteria among numerous defined operation scenarios of a microgrid or any power network.

Declaration of competing interest

No author associated with this paper has disclosed any potential or pertinent conflicts which may be perceived to have impending conflict with this work. For full disclosure statements refer to https://doi.org/10.1016/j.asoc.2020.106062.

Appendix A

See Tables A.1–A.9.

Appendix B

See Table B.1.

References

[1] B.J. Brearley, R.R. Prabu, A review on issues and approaches for microgrid protection, Renew. Sustain. Energy Rev. 67 (2017) 988–997.
[2] S.A. Hosseini, H.A. Abyaneh, S.H.H. Sadeghi, F. Razavi, A. Nasiri, An overview of microgrid protection methods and the factors involved, Renew. Sustain. Energy Rev. 64 (2016) 174–186.
[3] S. Kar, A comprehensive protection scheme for micro-grid using fuzzy rule base approach, Energy Syst. 8 (2017) 449–464.
[4] P.S. Georgilakis, N.D. Hatziargyriou, Optimal distributed generation placement in power distribution networks: models, methods, and future research, IEEE Trans. Power Syst. 28 (2013) 3420–3428.
[5] T.S. Ustun, C. Ozansoy, A. Zayegh, A central microgrid protection system for networks with fault current limiters, in: 2011 10th International Conference on Environment and Electrical Engineering, IEEE, 2011, pp. 1–4.
[6] A.A. Memon, K. Kauhaniemi, A critical review of AC microgrid protection issues and available solutions, Electr. Power Syst. Res. 129 (2015) 23–31.
[7] H.J. Laaksonen, Protection principles for future microgrids, IEEE Trans. Power Electron. 25 (2010) 2910–2918.
[8] M. Marzband, M.M. Moghaddam, M.F. Akorede, G. Khomeyrani, Adaptive load shedding scheme for frequency stability enhancement in microgrids, Electr. Power Syst. Res. 140 (2016) 78–86.
[9] H. Lin, J.M. Guerrero, J.C. Vásquez, C. Liu, Adaptive distance protection for microgrids, in: IECON 2015-41st Annual Conference of the IEEE Industrial Electronics Society, IEEE, 2015, pp. 000725–000730.
[10] H. Laaksonen, D. Ishchenko, A. Oudalov, Adaptive protection and microgrid control design for Hailuoto Island, IEEE Trans. Smart Grid 5 (2014) 1486–1493.
[11] H.M. Sharaf, H.H. Zeineldin, D.K. Ibrahim, E.L. Essam, A proposed coordination strategy for meshed distribution systems with DG considering user-defined characteristics of directional inverse time overcurrent relays, Int. J. Electr. Power Energy Syst. 65 (2015) 49–58.
[12] H.F. Habib, A.A.S. Mohamed, M. El Hariri, O.A. Mohammed, Utilizing supercapacitors for resiliency enhancements and adaptive microgrid protection against communication failures, Electr. Power Syst. Res. 145 (2017) 223–233.
[13] H.-C. Jo, S.-K. Joo, Superconducting fault current limiter placement for power system protection using the minimax regret criterion, IEEE Trans. Appl. Supercond. 25 (2015) 1–5.
[14] W. El-Khattam, T.S. Sidhu, Resolving the impact of distributed renewable generation on directional overcurrent relay coordination: a case study, IET Renew. Power Gener. 3 (2009) 415–425.
[15] M.A. Zamani, T.S. Sidhu, A. Yazdani, A protection strategy and microprocessor-based relay for low-voltage microgrids, IEEE Trans. Power Deliv. 26 (2011) 1873–1883.
[16] X. Li, A. Dyśko, G.M. Burt, Application of communication based distribution protection schemes in islanded systems, in: 45th International Universities Power Engineering Conference UPEC2010, IEEE, 2010, pp. 1–6.
[17] S.A.M. Javadian, M.R. Haghifam, S.M.T. Bathaee, M.F. Firoozabad, Adaptive centralized protection scheme for distribution systems with DG using risk analysis for protective devices placement, Int. J. Electr. Power Energy Syst. 44 (2013) 337–345.
[18] H.H. Zeineldin, H.M. Sharaf, D.K. Ibrahim, E.E.-D.A. El-Zahab, Optimal protection coordination for meshed distribution systems with DG using dual setting directional over-current relays, IEEE Trans. Smart Grid 6 (2014) 115–123.
[19] H.M. Sharaf, H.H. Zeineldin, E. El-Saadany, Protection coordination for microgrids with grid-connected and islanded capabilities using communication assisted dual setting directional overcurrent relays, IEEE Trans. Smart Grid 9 (2016) 143–151.
[20] M. Singh, T. Vishnuvardhan, S.G. Srivani, Adaptive protection coordination scheme for power networks under penetration of distributed energy resources, IET Gener. Transm. Distrib. 10 (2016) 3919–3929.
[21] Y. Zhang, J. Ma, J. Zhang, Z. Wang, Fault diagnosis based on cluster analysis theory in wide area backup protection system, in: 2009 Asia-Pacific Power and Energy Engineering Conference, IEEE, 2009, pp. 1–4.
[22] F.E. Perez, R. Aguilar, E. Orduna, J. Jäger, G. Guidi, High-speed non-unit transmission line protection using single-phase measurements and an adaptive wavelet: zone detection and fault classification, IET Gener. Transm. Distrib. 6 (2012) 593–604.
[23] M. Farhadi, O.A. Mohammed, A new protection scheme for multi-bus DC power systems using an event classification approach, IEEE Trans. Ind. Appl. 52 (2016) 2834–2842.
[24] J.M. Johnson, A. Yadav, Complete protection scheme for fault detection, classification and location estimation in HVDC transmission lines using support vector machines, IET Sci. Meas. Technol. 11 (2016) 279–287.
[25] M. Ojaghi, V. Mohammadi, Use of clustering to reduce the number of different setting groups for adaptive coordination of overcurrent relays, IEEE Trans. Power Deliv. 33 (2017) 1204–1212.
[26] MATLAB Version 9.5.0.944444 (R2018b), The MathWorks Inc., Natick, Massachusetts, 2018.
[27] DIgSILENT PowerFactory Version 15.1.7, DIgSILENT GmbH, Stuttgart, Germany, 2014.
[28] C.W. So, K.K. Li, Overcurrent relay coordination by evolutionary programming, Electr. Power Syst. Res. 53 (2000) 83–90.
[29] H.A. Abyaneh, M. Al-Dabbagh, H.K. Karegar, S.H.H. Sadeghi, R.A.J. Khan, A new optimal approach for coordination of overcurrent relays in interconnected power systems, IEEE Trans. Power Deliv. 18 (2003) 430–435.
[30] C. So, K. Li, Intelligent method for protection coordination, in: 2004 IEEE International Conference on Electric Utility Deregulation, Restructuring and Power Technologies. Proceedings, IEEE, 2004, pp. 378–382.
[31] F. Razavi, H.A. Abyaneh, M. Al-Dabbagh, R. Mohammadi, H. Torkaman, A new comprehensive genetic algorithm method for optimal overcurrent relays coordination, Electr. Power Syst. Res. 78 (2008) 713–720.
[32] J. Gholinezhad, K. Mazlumi, P. Farhang, Overcurrent relay coordination using MINLP technique, in: 2011 19th Iranian Conference on Electrical Engineering, IEEE, 2011, pp. 1–6.

[33] A. Korashy, S. Kamel, A.-R. Youssef, F. Jurado, Modified water cycle algorithm for optimal direction overcurrent relays coordination, Appl. Soft Comput. 74 (2019) 10–25.

[34] M.G.M. Zanjani, K. Mazlumi, I. Kamwa, Application of μPMUs for adaptive protection of overcurrent relays in microgrids, IET Gener. Transm. Distrib. 12 (2018) 4061–4068.

[35] B. Avşar, D.E. Aliabadi, Parallelized neural network system for solving Euclidean traveling salesman problem, Appl. Soft Comput. 34 (2015) 862–873.

[36] B. Jiang, L. Harrie, Selection of streets from a network using self-organizing maps, Trans. GIS 8 (2004) 335–350.

[37] T. Kohonen, The self-organizing map, Proc. IEEE 78 (1990) 1464–1480.

[38] A.K. Jain, J. Mao, K.M. Mohiuddin, Artificial neural networks: A tutorial, Computer 29 (1996) 31–44.

[39] T. Kohonen, Self-Organizing Maps, third ed., Springer-Verlag Berlin Heidelberg, 2001, http://dx.doi.org/10.1007/978-3-642-56927-2.

[40] P.K. Modi, S.P. Singh, J.D. Sharma, Fuzzy neural network based voltage stability evaluation of power systems with SVC, Appl. Soft Comput. 8 (2008) 657–665.

[41] J. Llanos, R. Morales, A. Núñez, D. Sáez, M. Lacalle, L.G. Marín, R. Hernández, F. Lanas, Load estimation for microgrid planning based on a self-organizing map methodology, Appl. Soft Comput. 53 (2017) 323–335.

[42] W.F.F. BaranM, F. WuF, Network reconfiguration in distribution systems for loss reduction and load balancing, IEEE Trans. PWRD 4 (1989) 1401–1407.

[43] S. Deb, K. Tammi, K. Kalita, P. Mahanta, Impact of electric vehicle charging station load on distribution network, Energies 11 (2018) 178.

[44] T. Sattarpour, M. Farsadi, Parking lot allocation with maximum economic benefit in a distribution network, Int. Trans. Electr. Energy Syst. 27 (2017) e2234.

[45] A. Stateczny, M. Wlodarczyk-Sielicka, Self-organizing artificial neural networks into hydrographic big data reduction process, in: Rough Sets and Intelligent Systems Paradigms, Springer, 2014, pp. 335–342.

[46] M. Wlodarczyk-Sielicka, A. Stateczny, Selection of SOM parameters for the needs of clusterization of data obtained by interferometric methods, in: 2015 16th International Radar Symposium, IRS, IEEE, 2015, pp. 1129–1134.

[47] S. Lloyd, Least squares quantization in PCM, IEEE Trans. Inf. Theory 28 (1982) 129–137.

[48] D. Arthur, S. Vassilvitskii, k-means++: The advantages of careful seeding, in: Society for Industrial and Applied Mathematics, pp. 1027–1035.